DOI: 10.1002/ejic.201000405

5-(2-Thienyl)tetrazolates as Ligands for Ru^{II}–Polypyridyl Complexes: Synthesis, Electrochemistry and Photophysical Properties

Stefano Stagni,*[a] Antonio Palazzi,[a] Pierpaolo Brulatti,[a][‡] Mauro Salmi,[a] Sara Muzzioli,[a] Stefano Zacchini,[a] Massimo Marcaccio,*[b] and Francesco Paolucci[b]

Keywords: Ruthenium / N ligands / Polypyridyl complexes / Thiophenes / Electrophilic addition / Cyclic voltammetry

In this contribution, we report the synthesis, the characterization and the study of the electrochemical and photophysical properties of some novel mononuclear Ru^{II}–polypyridyl complexes of the general formula $[Ru(tpy)(bpy)\mathbf{L}]^+$ (tpy = 2,2′:6′,2"-terpyridine, bpy = 2,2′-bipyridyl) in which **L** is represented by 5-(2-thienyl)tetrazolate-type ligands. In addition, the reactivity of these mononuclear species toward different electrophiles such as H^+ and CH_3^+ has been investigated, and the effects of the resulting regioselective electrophilic attacks on the electronic and structural properties of the tetrazolate ligand have been studied by NMR (^1H, ^{13}C) spectroscopy and X-ray crystal structural determination. Also, the electronic properties of the complexes have been explored by means of absorption and emission spectroscopy, together with a detailed electrochemical investigation combined with density functional theory (DFT) calculations. The data obtained from the study of such "model" mononuclear species constituted the basis for the characterization of the corresponding bithienyl-bridged dinuclear Ru^{II} complex, which displayed similar physical–chemical properties and an analogous behaviour toward the addition of electrophilic agents.

Introduction

Over the past three decades, the enormous scientific interest devoted to the investigation of Ru^{II}–polypyridyl complexes has been primarily driven by the opportunity of combining the peculiar photophysical and electrochemical properties exhibited by this class of coordination compounds.[1] In particular, the fundamental studies performed on these chemically stable and synthetically attractive molecules have prompted their application in a wide range of research fields[2] with regards to the design of photosensitizers for light-harvesting devices,[3] synthesis of electrochemiluminescent (ECL) molecules,[4] DNA photoprobing,[5] and photoactive units for light-driven catalysis.[6] A key factor for achieving a similar "technological versatility" has been provided by the chance of manipulating the photophysical features and the redox behaviours of Ru^{II}–polypyridyl complexes by performing modifications on the coordinated ligands. Accordingly, the scientific literature focussed on this kind of Ru^{II} compounds has evolved with the preparation of thousands of complexes; they differ either by the presence of various substituents on the backbone of the "classic" bpy- or tpy-type (bpy = 2,2′-bipyridyl, tpy = 2,2′:6′,2"-terpyridine) ligands or, for instance, by the use of different aromatic five-membered N-heterocycles for the construction of several polypyridine analogues.[1] Within this latter framework, we recently extended the family of Ru^{II}–polypyridyl complexes by introducing tetrazolate-type ligands [R–CN_4^-] into the Ru^{II} coordination sphere.[7] Despite their limited consideration for the design of similar metal complexes,[8] 5-substituted tetrazolates were shown to be interesting "actor" ligands for such molecular systems, as witnessed by the good photophysical performances displayed by some Ru^{II} complexes in which the side rings of bpy or tpy were modified by the introduction of one or two tetrazolate moieties, respectively.[7a,7d] Furthermore, in one of our previous papers, we unexpectedly found that a dinuclear complex formed by two Ru(tpy)(bpy) peripheral units connected by a phenyl-bistetrazolate spacer exhibits an electrochemiluminescence (ECL) response of magnitude comparable to that of $[Ru(bpy)_3]^{2+}$.[7b] These promising results encouraged the further extension of our studies on dinuclear Ru^{II}–tetrazolate complexes by changing the nature of the π-conjugated spacer with the introduction of a bithienyl unit. Indeed, oligothiophenes, in light of their fully planar structures, stability and ease of preparation, have gained a great importance in the design of electro- and photoactive materials such as organic light-emitting diodes and organic

[a] Dipartimento di Chimica Fisica ed Inorganica, Università di Bologna,
viale Risorgimento 4, 40136 Bologna, Italy
[b] Dipartimento di Chimica "G. Ciamician", Università di Bologna,
via Selmi 2, 40126, Bologna, Italy
E-mail: stefano.stagni@unibo.it
massimo.marcaccio@unibo.it
[‡] Current Address: Department of Chemistry, University Science Laboratories,
South Road, Durham, DH1 3LE, U.K

Supporting information for this article is available on the WWW under http://dx.doi.org/10.1002/ejic.201000405.

 © 2010 Wiley-VCH Verlag GmbH & Co. KGaA, Weinheim View this journal online at wileyonlinelibrary.com

field-effect transistors.[9] In addition, the combination of Ru^{II}–polypyridyl fragments with thiophene-based oligomers has led to mono- or multimetallic arrays that have proven useful for optoelectronic applications[9b,10] and for the design of highly efficient Ru^{II} sensitizers for dye-sensitized solar cells (DSSCs).[3d,11] In the present paper, we describe a new family of Ru^{II}–polypyridyl compounds (Scheme 1) that consists of one dinuclear bithienyl-bridged Ru^{II}–tetrazolate complex and of its mononuclear Ru^{II}–(thienyl)tetrazolate building blocks. The synthesis, characterization and investigation of the electrochemical and photophysical properties of both mononuclear and dinuclear species will be discussed in detail, together with the reactivity of all the new Ru^{II} species with electrophiles such as CH_3^+ and H^+, due to the multidentate character of the tetrazolate ring.

Results and Discussion

Syntheses

The thienyl tetrazoles employed in this work were all prepared by the 1,3-dipolar cyclization of the azide anion (N_3^-) onto the CN moiety of the appropriate nitrile precursors.[12a] Among the synthetic protocols for the preparation of tetrazoles available from the literature,[12b–12e] the one reported by Mitsui and coworkers was found to provide the desired products in acceptable to good yields.[12d] The synthesis of the bis-tetrazole **$TDTH_2$** required a preliminary step that consisted of the preparation of the starting nitriles by the Pd^0-mediated homocoupling of 5-bromo-2-thiophene carbonitrile.[13] Prior to complexation, all tetrazoles were converted into the corresponding tetrazolate salts by

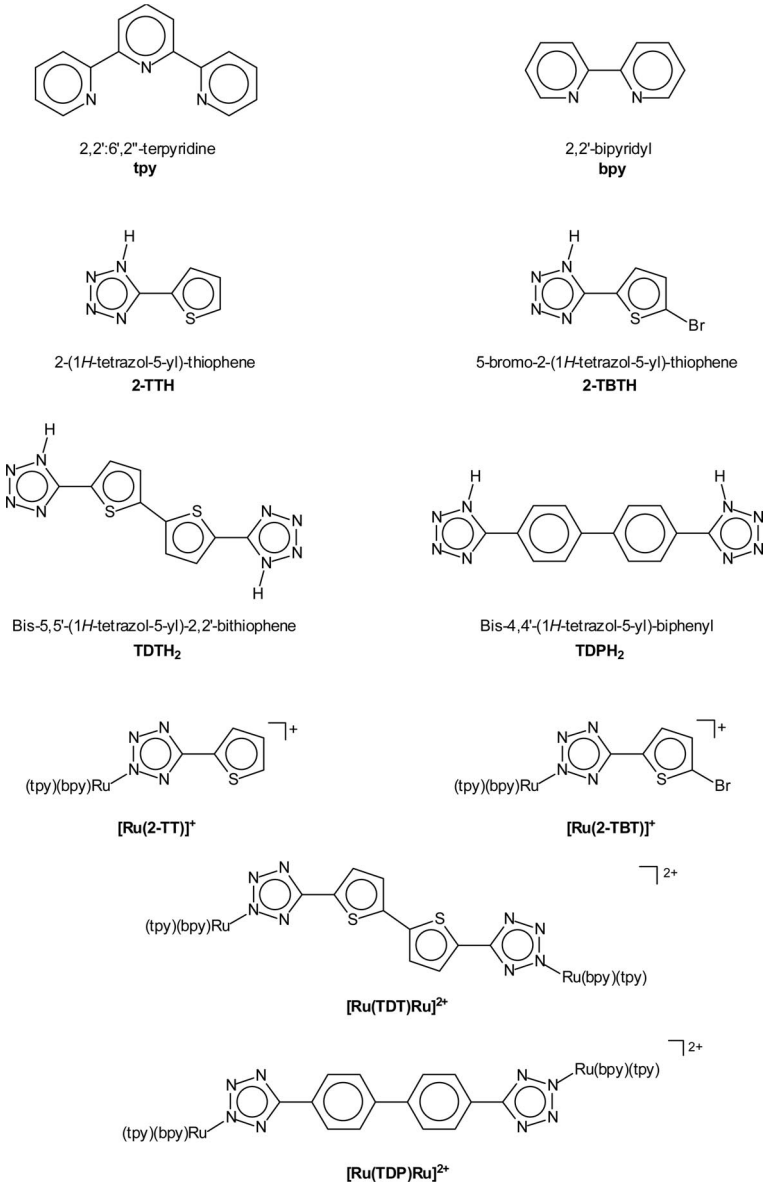

Scheme 1. Ligands, complexes and acronyms used in this work.

 © 2010 Wiley-VCH Verlag GmbH & Co. KGaA, Weinheim

their reaction with stoichiometric amounts of triethylamine. The synthetic procedure for the preparation of the target mono- and dinuclear complexes (Scheme 2) involved the preliminary reaction of the ruthenium precursor [Ru(tpy)(bpy)Cl][PF_6][14] with a slight molar excess amount of a silver salt (i.e., $AgPF_6$) in acetone heated to reflux. The removal of the precipitated AgCl afforded a deep red filtrate that probably contained the solvato complex [Ru(tpy)(bpy)(acetone)][PF_6]$_2$, which was thoroughly combined with a solution of the desired tetrazolate ligand in acetone. The reaction mixtures were stirred at reflux for 10–15 h and the target complexes were all purified by alumina-filled column chromatography. The preparation of the dinuclear complex **[Ru(TDT)Ru]$^{2+}$** was also attempted by performing the homocoupling reaction of the Br-containing compound **[Ru(2-TBT)]$^+$**,[2,15] thereby leading to the isolation of **[Ru(2-TT)]$^+$** as the only product. Further experiments devoted to the optimization of this latter procedure, which could represent a more convenient way for the preparation of similar Ru^{II} dinuclear species, are in progress. Also, in consideration of the presence of a pendant thienyl group, attempts toward the formation of dinuclear species by electrochemical polymerization[10e] of the corresponding mononuclear complexes are currently being pursued.

NMR Spectroscopy Studies

The complete NMR spectroscopic characterization of all the mononuclear and dinuclear species has been accomplished with the use of ^{1}H gs-COSY, ^{1}H,^{13}C gs-HSQC and ^{1}H,^{13}C gs-HMQC two-dimensional techniques. However, the evidence for the formation of the desired tetrazolate complexes was at first inferred from the analysis of the ^{1}H NMR spectra, in which the signal pattern of the (thienyl)tetrazolate moiety could be clearly distinguished from those of the ancillary polypyridyl ligands.

As reported in our previous papers,[7] ^{13}C NMR spectroscopy represents a useful tool for determining which coordination isomer is formed upon the reaction of tetrazolate salts with various metal precursors (Scheme 3).

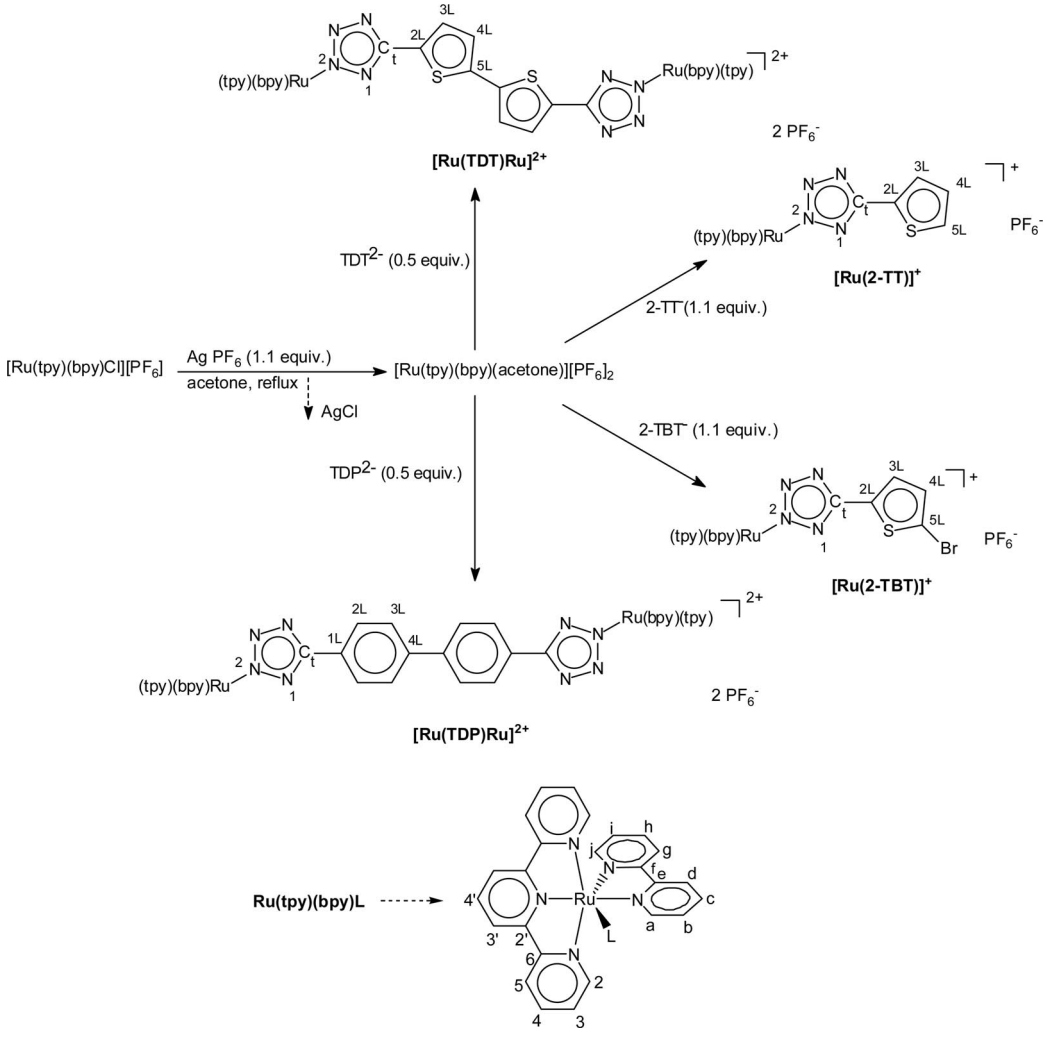

Scheme 2. Synthetic procedure adopted for the formation of all the complexes with atom labelling.

 © 2010 Wiley-VCH Verlag GmbH & Co. KGaA, Weinheim

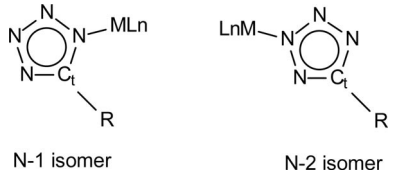

Scheme 3. N-1 and N-2 coordination isomers of tetrazolate complexes.

In the particular case of tetrazolates with six-membered aryl substituents, the exclusive coordination to the metal centre through the tetrazole N-2 position was witnessed by the tetrazole carbon (Ct) that resonates in the chemical-shift region between approximately δ = 161 and 165 ppm.[7b,16] Under the same experimental conditions, each of the mononuclear (thienyl)tetrazolate complexes **[Ru(2-TT)]$^+$** and **[Ru(2-TBT)]$^+$** display a single Ct signal that resonates within a narrow chemical-shift range centred at around δ = 160 ppm (Table 1). The close proximity of these values with those of the phenyl[7b,16a,16b] or pyridyl[16b] tetrazolate complexes we have reported recently, together with the significant upfield shift of the Ct resonance [$\Delta(\delta_{Ct}) \approx 8.0$ ppm], which is observed on going from the "free" (thienyl)tetrazole to the corresponding Ru^{II} complexes, suggest that the regioselective tetrazole 2-N complexation occurs also for (thienyl)tetrazolate complexes. This hypothesis is corroborated by the analysis of the molecular structure of the cationic species **[Ru(2-TT)]$^+$** and **[Ru(2-TBT)]$^+$**, which have been determined by using their **[Ru(2-TT)][PF$_6$]** and **[Ru(2-TBT)][PF$_6$]·2CH$_3$CN** salts (see Figures 1 and 2, Table 2). Both structures are composed of a Ru(tpy)(bpy) fragment to which a 5-thienyl-substituted tetrazolated ligand is N-2 coordinated. The bonding parameters for the former parallel very well the ones reported for other complexes that contain the Ru(tpy)(bpy) unit[17] and, in particular, the closely related [Ru(4-TBN)]$^+$ [TBN = 4-(5-tetrazolato)benzonitrile] analogue in which the same unit is bonded to a 5-phenyl-substituted tetrazolate.[7b] As expected in such complexes, the bond length of ruthenium to the central tpy nitrogen atom [Ru(1)–N(4) 1.958(4) and 1.957(3) Å for **[Ru(2-TT)]$^+$** and **[Ru(2-TBT)]$^+$**, respectively] is around 0.1 Å shorter than the other Ru–N distances [2.05–2.10 Å]. The tetrazolate rings in both cations are almost flat (mean deviations from the average least-square planes are 0.0013 Å for both molecules), as expected for aromatic cyclic compounds. The relative arrangement of the tetrazolate and thienyl ligands significantly differ in the two cations. Thus, the two five-membered rings are non-coplanar in **[Ru(2-TT)]$^+$** [dihedral angle N(6)–C(26)–C(27)–C(28) 162.3(5)°], whereas they are nearly coplanar in **[Ru(2-TBT)]$^+$** [dihedral angle N(6)–C(26)–C(27)–C(28) –172.0(4)°]. For comparison, in the analogous [Ru(4-TBN)]$^+$ it was found that the five-membered tetrazolate ring and the six-membered aryl ring formed a dihedral angle of +7.3(6)° and this was taken as informative for inter-ring conjugation within the ligand. In virtue of these three structures, the lack of coplanarity in **[Ru(2-TT)]$^+$** might be mainly ascribed to the presence of the five-membered thienyl ring, the effect of which is partially counterbalanced in **[Ru(2-TBT)]$^+$** by the presence of the bromine substituent.

Relative to the case of the dinuclear complex **[Ru(TDT)-Ru]$^{2+}$**, the analysis of both ^{1}H and ^{13}C NMR spectra provide evidence for the formation of a symmetrical species, as deduced from the presence of a number of signals equal to the half of the total protons or carbons of the entire molecule. In particular, the ^{13}C NMR spectrum displays a single tetrazole carbon resonance at around δ = 160 ppm to indi-

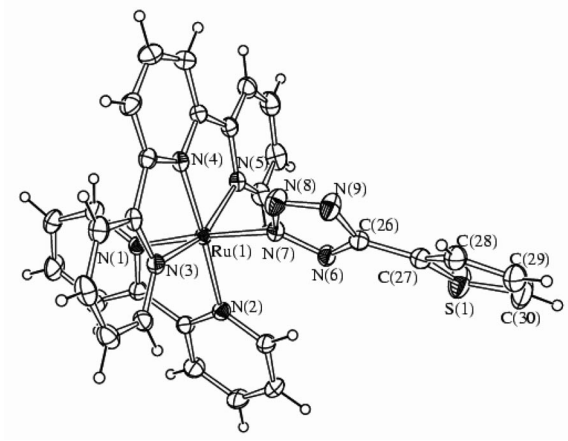

Figure 1. Molecular structure of the cation **[Ru(2-TT)]$^+$** with key atoms labelled. Displacement ellipsoids are at 30% probability level.

Table 1. Selected ^{1}H (400 MHz) and ^{13}C (75 MHz) NMR spectroscopic data (δ values) of all the ligands and complexes[a] reported in this paper. See Scheme 2 for atom labelling.

	C_t[b]	C-3L	C-4L	C-5L	H-3L	H-4L	H-5L
2-TTH	151.4	129.3	128.7	130.5	7.79	7.26	7.85
2-TBTH	151.3	132.2	130.1	116.2	7.41	7.30	–
TDTH$_2$	151.3	130.4	126.7	125.2	7.78	7.61	–
[Ru(2-TT)]$^+$	158.9	126.5	128.5	125.7	7.23–7.32	6.97	7.23–7.32
[Ru(2-TBT)]$^+$	159.8	125.9	131.1	112.5	7.03	6.98	–
[Ru(2-(H)TT)]$^{2+}$	152.7	131.5	129.7	132.6	7.65–7.71	7.11–7.18	7.65–7.71
[Ru(2-(Me)TT)]$^{2+}$	152.0	132.4	129.8	133.1	7.53	7.18	7.72
[Ru(2-(Me)TBT)]$^{2+}$	152.0	133.1	133.0	118.7	7.41–7.43	7.21	–
[Ru(TDT)Ru]$^{2+}$	160.1	125.1	126.4	132.4	7.14	7.04	–
[Ru(Me)(TDT)(Me)Ru]$^{4+}$	150.3	131.2	126.3	121.2	7.61	7.45	–

[a] Solvents employed: [D$_6$]DMSO for all ligands; CD$_3$CN for all the remaining species. All experiments were performed at r.t.; chemical shifts are expressed in ppm. [b] See Scheme 2 for atom labelling.

 © 2010 Wiley-VCH Verlag GmbH & Co. KGaA, Weinheim

Table 2. Selected bond lengths [Å] and angles [°] for **[Ru(2-TT)]$^+$**, **[Ru(2-TBT)]$^+$**, **[Ru(2-(H)TT)]$^{2+}$** and **[Ru(2-(Me)TT)]$^{2+}$**.

	[Ru(2-TT)]$^+$	[Ru(2-TBT)]$^+$	[Ru{2-(H)TT}]$^{2+}$	[Ru{2-(Me)TT}]$^{2+}$
Ru(1)–N(1)	2.058(3)	2.053(3)	2.042(3)	2.051(7)
Ru(1)–N(2)	2.097(4)	2.105(3)	2.085(3)	2.090(7)
Ru(1)–N(3)	2.064(3)	2.066(3)	2.066(3)	2.077(7)
Ru(1)–N(4)	1.958(4)	1.957(3)	1.969(3)	1.980(7)
Ru(1)–N(5)	2.075(3)	2.078(3)	2.066(3)	2.072(6)
Ru(1)–N(7)	2.097(3)	2.080(3)	2.099(3)	2.075(7)
N(6)–N(7)	1.351(5)	1.346(4)	1.341(4)	1.333(11)
N(7)–N(8)	1.296(5)	1.311(4)	1.288(4)	1.297(11)
N(8)–N(9)	1.341(5)	1.340(5)	1.327(4)	1.349(11)
N(9)–C(26)	1.322(6)	1.330(5)	1.342(5)	1.321(13)
C(26)–C(27)	1.465(6)	1.455(5)	1.441(5)	1.452(14)
C(27)–C(28)	1.365(7)	1.367(6)	1.379(6)	1.376(17)
C(28)–C(29)	1.410(8)	1.418(6)	1.382(7)	1.38(2)
C(29)–C(30)	1.325(9)	1.334(7)	1.298(9)	1.41(3)
C(27)–S(1)	1.712(5)	1.721(4)	1.708(4)	1.711(13)
C(30)–S(1)	1.715(7)	1.714(5)	1.696(5)	1.680(18)
C(30)–Br(1)	–	1.874(5)	–	–
N(9)–C(31)	–	–	–	1.455(14)
N(6)–N(7)–N(8)	111.0(3)	110.4(3)	112.3(3)	112.2(7)
N(7)–N(8)–N(9)	108.8(4)	109.4(3)	105.4(3)	105.2(8)
N(8)–N(9)–C(26)	104.7(4)	104.3(3)	109.5(3)	108.8(7)
N(9)–C(26)–N(6)	112.9(4)	112.8(3)	107.6(3)	108.7(8)
C(26)–N(6)–N(7)	102.6(4)	103.1(3)	105.2(3)	105.1(7)
C(28)–C(27)–S(1)	111.1(4)	111.1(3)	110.6(3)	111.7(10)
C(27)–S(1)–C(30)	91.3(3)	90.9(2)	90.6(3)	92.6(9)
C(29)–C(30)–S(1)	112.1(5)	113.3(4)	113.1(4)	110.0(12)
C(28)–C(29)–C(30)	113.3(5)	111.9(4)	114.1(4)	113.7(15)
C(27)–C(28)–C(29)	112.2(5)	112.8(4)	111.6(4)	111.6(16)

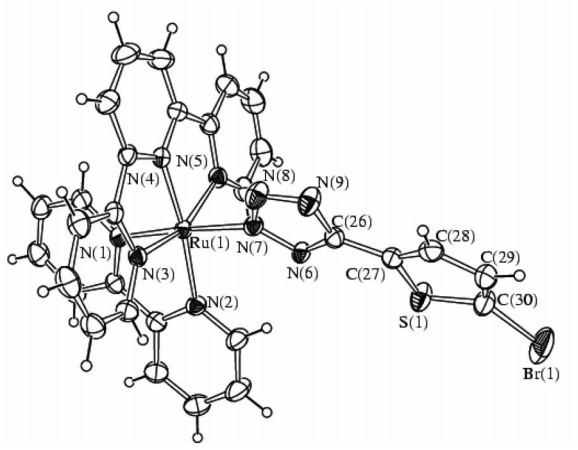

Figure 2. Molecular structure of the cation **[Ru(2-TBT)]$^+$** with key atoms labelled. Displacement ellipsoids are at 30% probability level.

cate that, in analogy with the mononuclear complexes **[Ru(2-TT)]$^+$** and **[Ru(TBT)]$^+$**, each of the peripheral tetrazolate rings is coordinated to the metal fragment through the tetrazole N-2 atom.

Addition of Electrophiles

Among the features of metal–tetrazolate complexes, one of the most important is represented by the chance of performing electrophilic additions onto the coordinated five-membered ring. This is made possible by the presence of three imine-type nitrogen atoms, all of which are, in principle, susceptible to electrophilic attack. In our previous studies, we demonstrated that the reaction of Fe^{II} or Ru^{II} 5-aryltetrazolate mononuclear complexes with equimolar amounts of methyl triflate or triflic acid led to the formation of one methylated or protonated product, respectively.[7b,14] In all cases, the electrophilic attack was found to occur regioselectively at the N-4 atom of the tetrazole ring, the position which less suffers from the steric encumbrance of the metal fragment. This latter feature was at first deduced from the analysis of the ^{13}C NMR spectra of the product complexes, which displayed one single tetrazole carbon signal that resonated in a chemical-shift range (for C_t, δ = 155–157 ppm) that was markedly different from those typical of the cationic precursors (for C_t, δ = 162–164 ppm). An almost analogous behaviour is observed when the Ru^{II}–thienytetrazolate mononuclear complexes reported in this work were treated with 1:1 stoichiometric amounts of the same sources of CH_3^+ or H^+ (Scheme 4).

The resulting bis-cationic species **[Ru{2-(Me)TT}]$^{2+}$**, **[Ru{2-(H)TT}]$^{2+}$** and **[Ru{2-(Me)TBT}]$^{2+}$** all displayed one tetrazole carbon resonance upfield-shifted by about δ = 7.0 ppm with respect to that observed for the starting **[Ru(2-TT)]$^+$** and **[Ru(2-TBT)]$^+$**, respectively. In analogy with our past studies, the electrophilic attack likely occurs at the N-4 tetrazole atom (see Scheme 4 for numbering), this latter evidence being further corroborated by the analysis of the crystal structure of the methylated species **[Ru{2-(Me)TT}]$^{2+}$** and of the protonated complex **[Ru{2-(H)-**

 © 2010 Wiley-VCH Verlag GmbH & Co. KGaA, Weinheim

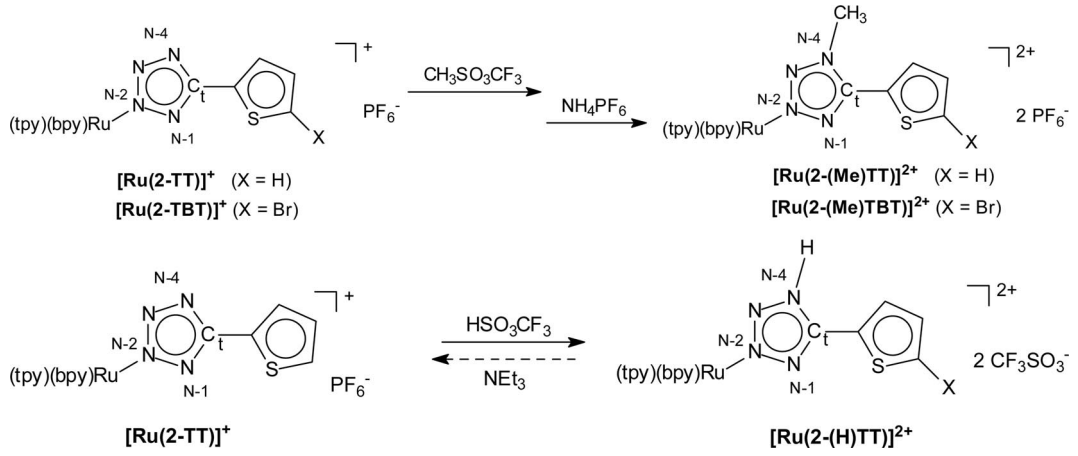

Scheme 4. Methylation (top) and protonation (bottom) reactions of mononuclear Ru^{II}–(thienyl)tetrazolate complexes.

TT}]$^{2+}$, as determined from their **[Ru{2-(H)TT}][CF_3SO_3]$_2$·CH_3CN** and **[Ru{2-(Me)TT}][PF_6]$_2$·2CH_3CN** salts (Figure 3, Figure 4 and Table 2). Hydrogen bonding is present in the crystal of **[Ru{2-(H)TT}][CF_3SO_3]$_2$·CH_3CN**; it involves one $CF_3SO_3^-$ anion and the N–H tetrazolate group [N(9)···O(1) 2.697(5) Å, N(9)–H(90) 0.852(19) Å, H(90)···O(1) 1.86(2) Å, N(9)–H(90)···O(1) 167(5)°]. As previously found for **[Ru(4-TBN)]$^+$**,[7b] both protonation and methylation occur on N(9) [N-4 following tetrazole-ring nomenclature] and do not significantly affect the bonding parameters of the complexes. The most significant difference is found on the dihedral angles between the two five-membered rings that were non-coplanar in the parent **[Ru(2-TT)]$^+$** cation [N(6)–C(26)–C(27)–C(28) –162.3(5)°], whereas they become almost coplanar in the **[Ru{2-(Me)TT}]$^{2+}$** and **[Ru{2-(H)TT}]$^{2+}$** bis-cations [N(6)–C(26)–C(27)–C(28) –174.1(13) and 177.8(5)°, respectively]. This behaviour is the exact opposite of what was found in [Ru(4-TBN)]$^+$, which contained a six-membered aryl ring bonded to the tetrazolate ligand instead of the five-membered thienyl ring. For this, the almost coplanar arrangement of the two rings found in the [Ru(4-TBN)]$^+$ monocation [dihedral 7.3(6)°] was completely disrupted after methylation [dihedral 118.9(6)°], whereas the protonated analogous displayed an intermediate behaviour [dihedral 24.6(11)°] by dint of the smaller steric hindrance of the hydrogen atom compared to the methyl group. In the present case, the similar structures assumed by the methylated and protonated species, that is, **[Ru{2-(Me)TT}]$^{2+}$** and **[Ru{2-(H)TT}]$^{2+}$**, is probably a consequence of the presence of the less sterically demanding thienyl ring. The steric as well as electronic properties of this five-membered ring might also account for the opposite trends of inter-ring dihedral angles with respect to the aryl-substituted analogues [Ru(4-TBN)]$^+$, [Ru{4-(H)TBN}]$^{2+}$ and [Ru{4-(Me)TBN}]$^{2+}$.[7b] Finally, considering also the bromine-derivative **[Ru(2-TBT)]$^+$**, it may be concluded that either substitution on the tetrazolate or the thienyl ring considerably affect the inter-ring dihedral angles in 5-thienyl-substituted tetrazolate complexes, in which the nonsubstituted ligand is non-coplanar, whereas it becomes almost coplanar after substitution. The only striking difference with respect to the previously reported species[7b,14c] is represented by the substantial coplanarity of the methylated or protonated tetrazolate and the thiophene rings, the reduced ring size of the thienyl unit being the key factor for determining a similar geometry. Also, it is worth noting that the protonation reaction maintains its reversible character, as previously documented for a number of 5-aryl tetrazolate complexes. Indeed, the addition of one equivalent of triethyl amine to the protonated species **[Ru{2-(H)TT}]$^{2+}$** causes the quantitative formation of the cationic precursor **[Ru(2-TT)]$^+$** (see Scheme 4).

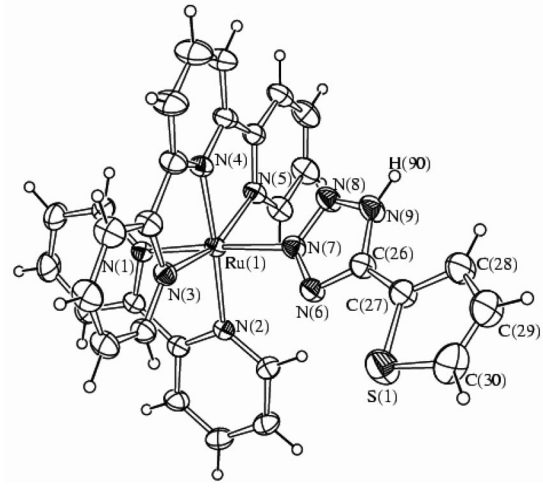

Figure 3. Molecular structure of the cation **[Ru{2-(H)TT}]$^{2+}$** with key atoms labelled. Displacement ellipsoids are at 30% probability level.

Relative to the bithienyl linked dinuclear complex **[Ru(TDT)Ru]$^{2+}$**, the methylation reaction was performed by adding two molar equivalents of methyl triflate to the starting compound. (Scheme 5).

The ^{1}H and ^{13}CNMR spectra of the resulting bis-methylated species displayed a number of resonances equal to half of the total protons and carbons of the molecule, which indicates that the double methylation reaction did not alter

 © 2010 Wiley-VCH Verlag GmbH & Co. KGaA, Weinheim

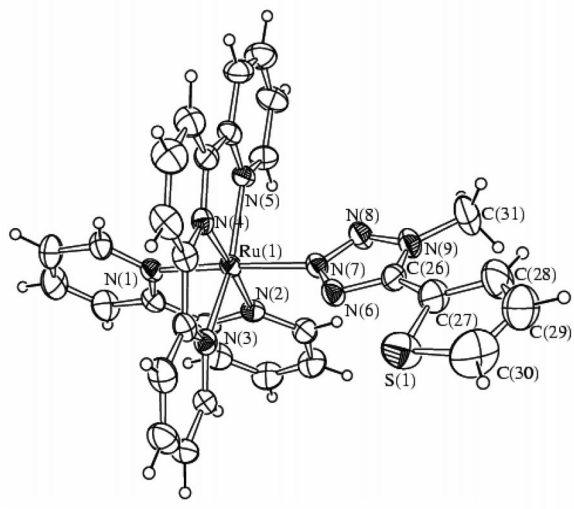

Figure 4. Molecular structure of the cation **[Ru{2-(Me)TT}]$^{2+}$** with key atoms labelled. Displacement ellipsoids are at 30% probability level.

the symmetry of the bis-tetrazolate bridging ligand. In addition, methylation was found to occur with the same regioselectivity as that observed in the case of the mononuclear **[Ru{2-(Me)TT}]$^{2+}$**. This latter feature was evidenced from the analysis of the ^{13}C NMR spectrum of **[Ru(Me)-(TDT)(Me)Ru]$^{4+}$**, which displayed one tetrazole carbon that resonated at a chemical-shift value ($\delta \approx 150$ ppm) significantly upfield-shifted with respect to that of the starting **[Ru(TDT)Ru]$^{2+}$**(Scheme 5).

Electrochemistry

The redox behaviour of the complexes was investigated in acetonitrile by cyclic voltammetry (CV) at room temperature using both platinum and glassy carbon as working electrodes. All potentials are collected in Table 3. It is well established that the redox processes in Ru^{II}–polypyridine complexes are mainly localized either on the metal centre (oxidations) or on the ligands (reductions).[18] In particular, all the mononuclear species **[Ru(2-TT)]$^{+}$** (Figure 5, a), **[Ru(2-TBT)]$^{+}$**, **[Ru{2-(Me)-TT}]$^{2+}$** and **[Ru{2-(Me)-TBT}]$^{2+}$** exhibited in the region of the positive potentials a single and reversible one-electron process, which can be confidently attributed to the oxidation of the Ru^{II} centre. In the case of the cationic compounds **[Ru(2-TT)]$^{+}$** and **[Ru(2-TBT)]$^{+}$**, the Ru^{II}-centred processes were found in a very narrow potential range ($E_{1/2}$ = 1.01 and 0.99 V for **[Ru(2-TT)]$^{+}$** and **[Ru(2-TBT)]$^{+}$**, respectively; see Table 3), which indicates the almost negligible influence that arises from the presence of a bromine substituent on the thiophene ring. On the other hand, a significant shift to higher potentials of the oxidation process is observed upon methylation of the complexes **[Ru(2-TT)]$^{+}$** and **[Ru(TBT)]$^{+}$** (i.e., **[Ru{2-(Me)TT}]$^{2+}$** and **[Ru{2-(Me)TBT}]$^{2+}$**species). On the basis of the redox behaviour and the electronic structure of the analogue ruthenium(II)–tetrazolate complexes, such a positive shift value can be mostly attributed to the increased charge of the bis-cationic methylated complex. However, examination of the quantum-chemical DFT calculations[19,20] shows that the highest occupied molecular orbital (HOMO) is mainly centred on Ru^{II}, but a non-negligible contribution comes from the tetrazole ring (Figure 6). Thus, the intro-

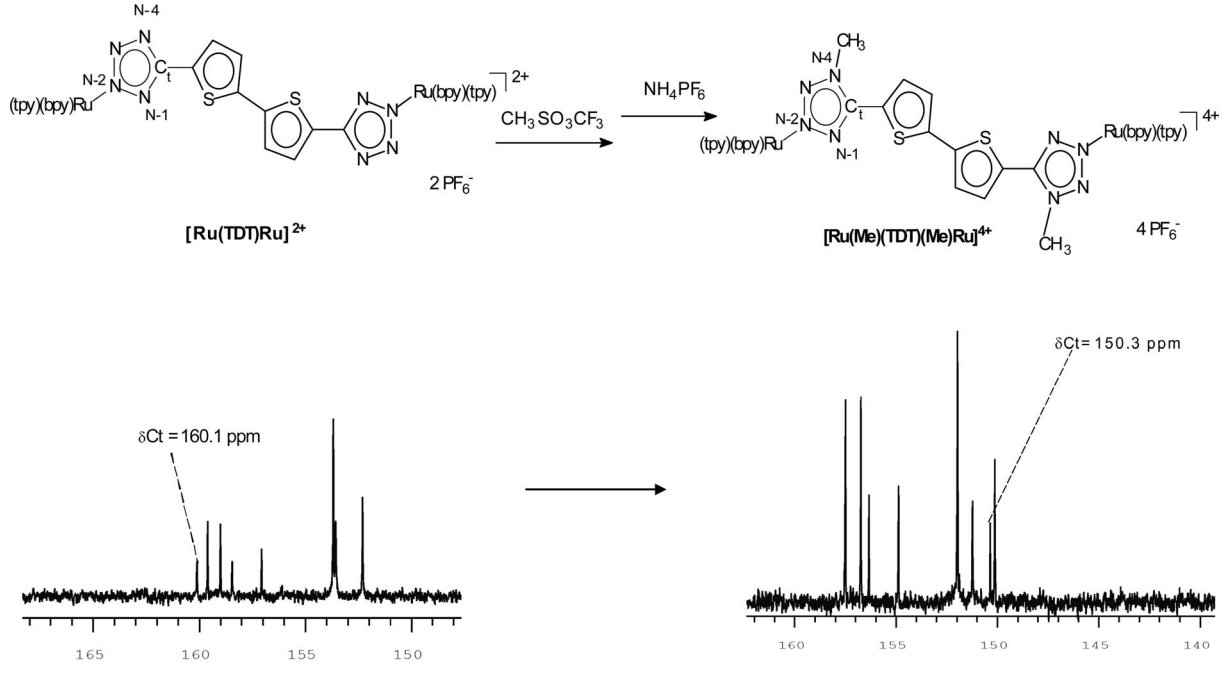

Scheme 5. Methylation of **[Ru(TDT)Ru]$^{2+}$** (top) and corresponding downfield shifting of the Ct resonance (bottom).

 © 2010 Wiley-VCH Verlag GmbH & Co. KGaA, Weinheim

duction of the methyl on the tetrazole ligand electronically perturbs the HOMO itself. This is also in line with the electrochemical findings, which show that methylation moves the oxidation processes to more positive potentials by an average value (around 300 mV) that is about twice the shift to less negative potentials observed for the reductions (see Table 3). Moreover, the oxidations are electron transfers that are somewhat more sluggish than the reductions (centred on the polypyridyl ligands); this is most probably associated with the higher reorganization energy related to the tetrazolate ligand involved in the oxidation process. Concerning the reductions, the CV investigation has been carried out by exploring the first processes, in particular those that occur within the potential window down to about –2.0 V (see Figure 5, a).

Table 3. Half-wave ($E_{½}$) redox potentials[a] (vs. SCE) of all complexes at 25 °C.

	$E_{½}$ (ox.) [V]		$E_{½}$ (red.) [V]	
Species	(1)	(2)	I	II
[Ru(2-TT)]$^+$	0.99		–1.42	–1.71
[Ru{2-(Me)TT}]$^{2+}$	1.30		–1.29	–1.57
[Ru(2-TBT)]$^+$	1.01		–1.42	–1.66[b]
[Ru{2-(Me)TBT}]$^{2+}$	1.28		–1.29	–1.59
[Ru(TDT)Ru]$^{2+}$	0.99	1.35	–1.39	–1.68
	1.02		–1.44	–1.72
[Ru(Me)(TDT)(Me)Ru]$^{4+}$	1.25		–1.31	–1.56[b]
	1.30		–1.39	
[Ru(TDP)Ru]$^{2+}$	1.01		–1.39	–1.70
	1.03		–1.44	–1.74
[Ru(Me)(TDP)(Me)Ru]$^{4+}$	1.24		–1.27	–1.55
	1.29		–1.32	–1.59

[a] In 0.1 M TBAH/CH_3CN. [b] Irreversible process; cathodic peak potential.

On the basis of the homologue species previously investigated[7b] and the DFT calculations, the various processes are localized on the two polypyridine ligands and, in particular, the first to be reduced is the tpy and then the bpy (Figure 6). Except for species **[Ru(2-TBT)]$^+$**, all the mononuclear complexes **[Ru(2-TT)]$^+$**, **[Ru{2-(Me)TT}]$^{2+}$** and **[Ru{2-(Me)TBT}]$^{2+}$** display two one-electron reversible voltammetric waves. The complex **[Ru(2-TBT)]$^+$** has the second one-electron reduction affected by a chemical irreversibility, most probably due to the presence of a Br on the (thienyl)-tetrazolate ligand. By observing the first reduction potentials, reported in Table 3, for the four mononuclear complexes it is possible to group them into two values: –1.42 V for the cationic pristine species and –1.29 V for the corresponding methylated species **[Ru{2-(Me)-TT}]$^{2+}$** and **[Ru{2-(Me)TBT}]$^{2+}$**.

The dinuclear species **[Ru(TDT)Ru]$^{2+}$** displays a voltammetric curve (Figure 5, b and Figure S4 in the Supporting Information) that consists of four distinct voltammetric peaks, three of which − two reductions and the first oxidation − are two one-electron processes with very close potentials, as evidenced by chronoamperometry. Such processes are found at almost the same values as the corresponding ones for the mononuclear building block **[Ru(2-TT)]$^+$**. The second oxidation peak is a one-electron process,

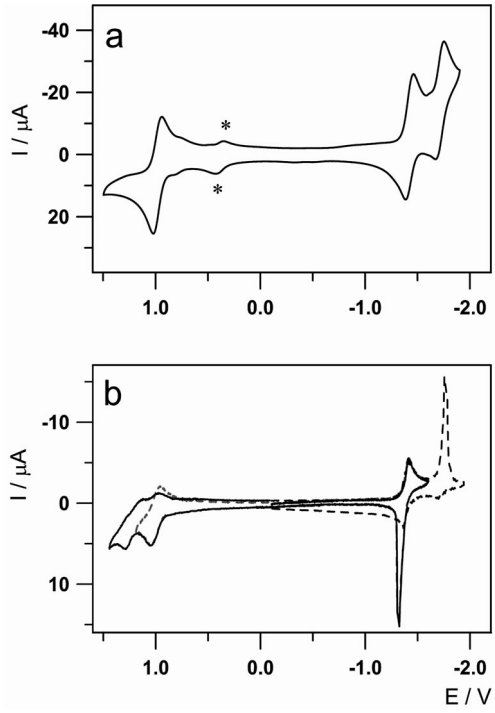

Figure 5. Cyclic voltammetric curves recorded in 0.07 M TBAH/CH_3CN, T = 25 °C, of (a) 1.5 mM mononuclear species **[Ru(2-TT)]$^+$**, working electrode glassy carbon disk (3 mm diameter), scan rate 0.1 V s^{-1}; and (b) 0.5 mM dinuclear complex **[Ru(TDT)Ru]$^{2+}$**, working electrode platinum disk (0.5 mm diameter), scan rate 0.2 V s^{-1}. In (a), the small voltammetric wave labelled by asterisks (*) is due to ferrocene added as internal standard (see the Experimental Section).

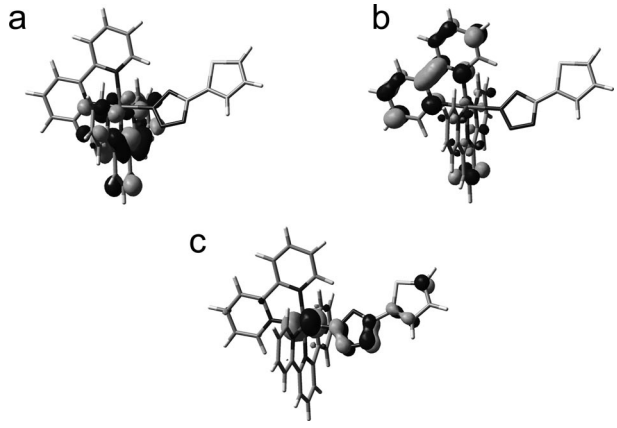

Figure 6. Molecular orbital surfaces of **[Ru(2-TT)]$^+$** showing the frontier orbitals involved in the first redox processes. (a) LUMO (first reduction) centred on the tpy; (b) LUMO + 1 (second reduction) centred on the bpy; (c) HOMO (oxidation) mainly centred on the ruthenium and partially on the coordinated tetrazole.

as it is half the height of the others, and it is affected by a follow-up chemical reaction that makes the first oxidation voltammetric peak less reversible on the reverse scan. It should be noted that higher-quality results were obtained by using a glassy carbon electrode. In fact, especially with this dinuclear complex, by using platinum as the electrode and strictly aprotic conditions, the reductions in acetonitrile

 © 2010 Wiley-VCH Verlag GmbH & Co. KGaA, Weinheim

solution are severely affected by strong adsorption phenomena, which disappear with the glassy carbon electrode and when the experiments are performed in less dry conditions. By taking into account the data reported for similar bithienyl or oligothienyl-bridged Ru^{II} dinuclear systems,[21,10b–10e] the fourth voltammetric wave, the one centred at 1.35 V (see Table 3), can be confidently attributed to a bridging-ligand-centred oxidation. This is also consistent with the number of electrons exchanged. Further support to this attribution is provided by the analysis of the voltammetric curve of the bis-methylated species **[Ru(Me)(TDT)-(Me)Ru]$^{2+}$**, which displays, in the positive potentials window, one single and reversible voltammetric peak (containing two close one-electron processes) that occurs, as expected, at more positive potentials than the first one observed for the bis-cationic precursor **[Ru(TDT)Ru]$^{2+}$**. In addition, the not innocent role played by the bridging ligand is evidenced by the comparison of the electrochemical features of the complex **[Ru(TDT)Ru]$^{2+}$** with those of the biphenyl-bridged dinuclear complex **[Ru(TDP)Ru]$^{2+}$**, which was prepared in an identical manner to **[Ru(TDT)Ru]$^{2+}$**. The dinuclear species **[Ru(TDP)Ru]$^{2+}$** displays a CV curve that consists of three voltammetric peaks: two in the negative potentials region and one on the positive side. The peaks are found at almost the same potential values of those determined for the corresponding processes of the mononuclear (thienyl)tetrazolate species **[Ru(2-TT)]$^{+}$**. All the voltammetric peaks are made up of two closely spaced one-electron processes, as obtained by chronoamperometric measurements, and this can be rationalized by the symmetry of the species and the fact that the electronic conjugation through the bis-phenylene bridging moiety is not very effective. This is in agreement with the electrochemical behaviour of a homologue species previously studied and the results of the quantum calculations performed.[7b] The potentials of the closely spaced processes have been determined by digital simulation of the voltammetric curves recorded at different scan rates. Thus, the two oxidations are localized on the two metal centres, the first two reductions (contained in the first peak) centred on the two tpy ligands and the last two reductions on the bpy ligands. When **[Ru(TDP)Ru]$^{2+}$** is treated with two equivalents of methyl triflate to afford the bis-methylated species **[Ru(Me)(TDP)-(Me)Ru]$^{4+}$**, the electrochemical behaviour shows a change in the potentials of the processes, similarly to that observed for the mononuclear **[Ru(2-TT)]$^{+}$**, but not in the morphology of the voltammetric curve. As expected, the oxidations move about 300 mV toward more positive potentials and the reduction becomes about 130 mV less negative with respect to the corresponding process of pristine **[Ru(TDP)Ru]$^{2+}$**.

Electronic Spectra

In Table 4, we report the absorption spectra of solutions of all complexes recorded in acetonitrile. The spectra show the expected features of most Ru-based metal complexes, with intense transitions at high energy (200–350 nm) and weaker bands in the visible region (400–600 nm). The series of bands in the UV range can be assigned to ligand-centred $\pi \rightarrow \pi^*$ (^{1}LC) absorptions, whereas the transitions observed in the visible part of the spectrum ($\varepsilon = (5–20) \times 10^3$ $M^{-1}cm^{-1}$) are assigned to singlet and triplet metal-to-ligand charge-transfer (^{1}MLCT and ^{3}MLCT, respectively) processes. The addition of electrophiles (CH_3^+ or H^+) to the complexes reported here results in the formation of species with increased positive charge, as evidenced by blueshift of the absorption maximum of the MLCT-based transition observed upon going from the starting compounds (i.e., **[Ru(2-TT)]$^{+}$**, **[Ru(2-TBT)]$^{+}$** and **[Ru(TDT)Ru]$^{2+}$**) to the corresponding methylation or protonation products (Figure 7).

As might be expected from Ru^{II}–tpy-based complexes, all the species reported here are almost not luminescent in acetonitrile at 298 K, with emission lifetimes shorter than 30 ns (Table 4) and almost undetectable emission quantum yields ($\phi < 0.001$ in all cases). As the consequence of the rigidochromic effect, the broad emissions centred in the wavelength range between 675 and 680 nm turn into slightly blueshifted and structured profiles when the analyses were performed on samples frozen at 77 K (Figure 8 and Figures S7 and S8 in the Supporting Information). The excitation spectra (Figures S9–S11 in the Supporting Infor-

Table 4. Absorption and emission spectral data of the (thienyl)tetrazolate complexes.

	Absorption[a]		Emission[b] (298 K)		Emission[b] (77 K)[c]	
Species	λ_{max} [nm] ($\varepsilon \times 10^4$ [$M^{-1}cm^{-1}$])	λ [nm]	τ [ns] (deaerated)	τ [ns] (air)	λ [nm]	τ [μs]
[Ru(2-TT)]$^{+}$	274 (4.24), 281 (4.27), 290sh (3.89) 312 (2.66), 352sh (0.52), 480 (0.62)	680	18.64	14.83	657	3.13
[Ru{2-(Me)TT}]$^{2+}$	273sh (3.51), 286 (4.00), 307 (3.32), 329sh (1.55), 460 (0.84)	680	22.10	18.11	647	2.98
[Ru{2-(H)TT}]$^{2+}$	242 (3.10), 254 (2.97), 286 (4.50), 307 (3.45), 465 (0.94)	675	18.44	18.23	644	4.20
[Ru(2-TBT)]$^{+}$	274sh (3.51), 282 (3.73), 292 (4.12), 312 (3.45), 357sh (0.48), 484 (0.75)	677	15.79	15.00	651	4.62
[Ru(Me)(2-TBT)]$^{2+}$	241 (2.45), 285 (3.82), 307 (3.20), 403sh (0.43), 461 (0.80)	n.d.[d]	–	–	–	–
[Ru(TDT)Ru]$^{2+}$	273(6.11), 311sh (1.91), 356 (0.49) 484 (0.30)	680	19.34	21.15	664	6.55
[Ru(Me)(TDT)(Me)Ru]$^{4+}$	237 (1.84), 271sh (2.19), 286 (2.71), 306 (2.61), 327sh (1.70) 353 (1.20), 403 (0.86), 456 (0.67)	675	22.15	19.13	665	4.72

[a] In air-equilibrated acetonitrile. [b] Excitation wavelength (λ) = 460 nm. [c] In butyronitrile glass. [d] n.d. = not detected.

 © 2010 Wiley-VCH Verlag GmbH & Co. KGaA, Weinheim

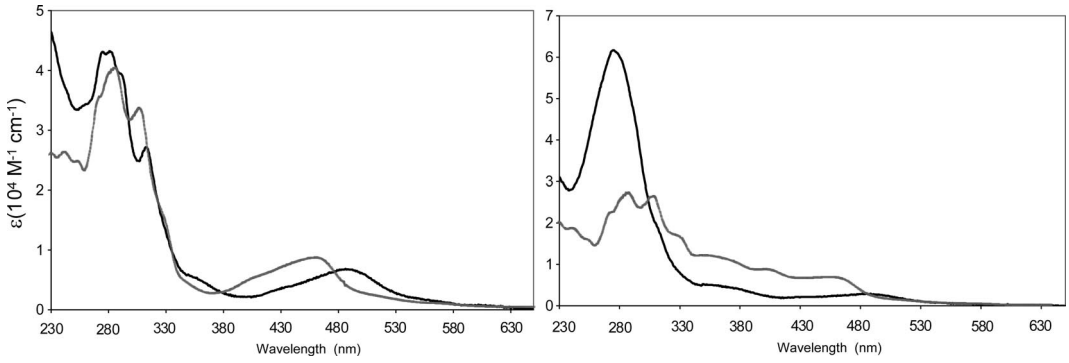

Figure 7. Absorption spectra of **[Ru(2-TT)]$^+$** (left, black trace) **[Ru{2-(Me)TT}]$^{2+}$** (left, grey trace), **[Ru(TDT)Ru]$^{2+}$** (right, black trace) and **[Ru(Me)(TDT)(Me)Ru]$^{4+}$** (right, grey trace).

mation) recorded on the frozen mononuclear species were not decisive enough to completely ascertain the nature of the multiple emission maxima (i.e., the presence of impurities or different emissive levels) that were observed in the corresponding emission spectra.

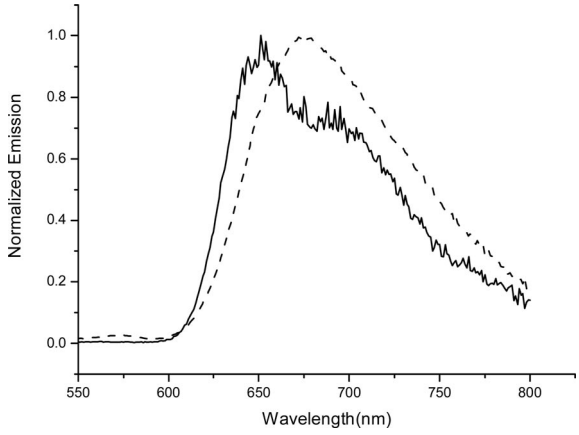

Figure 8. Normalized emission spectra **[Ru(2-TBT)]$^+$** in acetonitrile at room temperature (dotted line) and at 77 K (continuous line). Excitation wavelength: 460 nm.

At odds with the Ru^{II}–tetrazolate complexes we have reported so far, the addition of electrophiles to the mono- or dinuclear Ru^{II}–(thienyl)tetrazolate complexes **[Ru(2-TT)]$^+$** and **[Ru(TDT)Ru]$^{2+}$** did not result in any appreciable variation of the photophysical performance, as the probable consequence of the very poor emissive properties of the starting complexes.

Conclusion

The inclusion of the tetrazolate group (–CN_4^-) into the structure of thienyl- or bithienyl-based ligands reported in this paper introduces some interesting features into the chemistry of the corresponding Ru^{II}–polypyridyl complexes. First, the anionic character of the tetrazolate moiety ensures the strong binding to the metal centre. Also, because the coordination of the (thienyl)tetrazolates to the Ru^{II} centre occurs regioselectively through the N-2 position of the tetrazolate ring, the formation of any further coordination isomers is avoided. As reported for Fe^{II} and Ru^{II} 5-phenyl and 5-pyridyltetrazolate derivatives, an additional value that arises from the presence of a –CN_4^- group is given by the possibility of performing chemo- and regioselective electrophilic additions onto the resulting metal–tetrazolate complexes, thereby introducing the chance of permanently or reversibly modifying the structural and the electronic properties of the complexes by means of a methylation reaction or protonation–deprotonation mechanism, respectively. An almost analogous behaviour was observed also for the mononuclear Ru^{II}–(thienyl)tetrazolate complexes herein described, apart from the fact that, as deduced from the analysis of the resulting X-ray crystal structures, the methylation or protonation of the (thienyl)tetrazolate moiety did not involve any distortion from the coplanar arrangement of the five-membered aromatic rings. On the basis of closely similar spectroscopic, electronic and redox properties, these issues could be transferred from the "model" mononuclear species to the corresponding dinuclear bithienyl-bridged Ru^{II} complex, including the same "electrophile sensitivity" displayed by its mononuclear building blocks. Relative to the Ru^{II} dinuclear complex, the presence of "electronic communication" between the metal centres was not detected, the analysis of the electrochemical properties being indicative of the presence of a bithienyl-centred redox process rather than the formation of a Ru^{II}–Ru^{III} mixed-valence species. From the point of view of the luminescence properties, the detection of emitting processes was in all cases severely limited by the poor emissive performances of the Ru(tpy)(bpy) fragment. To overcome this problem and in consideration of the fact that thienyl tetrazolates might be viewed as interesting candidates for their incorporation into mono- or multimetallic assemblies characterized by peculiar and tunable electrochemical and photophysical properties, we are currently engaged in the preparation of a series of analogous Re^{I}-based compounds with enhanced light-emission performance.

Experimental Section

Materials: All reactions were routinely carried out under an argon atmosphere and by using standard Schlenk techniques. Solvents were distilled immediately before use under nitrogen from appropri-

 © 2010 Wiley-VCH Verlag GmbH & Co. KGaA, Weinheim

ate drying agents. Unless otherwise stated, chemicals were obtained commercially (e.g., Aldrich) and used without any further purification. [Ru(tpy)Cl_3],[22] [Ru(tpy)(bpy)Cl][PF_6],[14] 5,5′-(2,2′-bithiophene)dicarbonitrile and 4,4′-biphenyldicarbonitrile were prepared according to literature methods.[13] Relative to the description of the ^1H and ^{13}C NMR spectra (see below), the atom numbering[17c] is always made with reference to Scheme 2. Throughout this paper, the percentage yields of the product complexes are referenced to the molar quantity of the starting [Ru(tpy)(bpy)Cl][PF_6].

Warning! *Tetrazole derivatives are used as components for explosive mixtures.[12a] In this laboratory, the reactions described here were run using only a few grams and no problems were encountered. However, great caution should be exercised when handling or heating compounds of this kind.*

Instrumentation and Procedures: All the obtained complexes were characterized by elemental analysis and spectroscopic methods. Elemental analyses were performed with a ThermoQuest Flash 1112 Series EA instrument. Mass spectra were performed with a Waters ZQ-4000 instrument (ESI-MS, acetonitrile as the solvent) or with a Thermo Finnigan MAT 95 XP apparatus (EIMS). The routine NMR spectra (^1H, ^{13}C) were always recorded with a Varian Mercury Plus 400 instrument (^1H, 400.1 MHz; ^{13}C, 100.0 MHz). The spectra were referenced internally to residual solvent resonance, and were recorded at 298 K for characterization purposes. Bidimensional ^1H,^{13}C correlation spectra were measured by means of gs-HSQC and gs-HMBC experiments,[23] whereas ^1H,^1H correlations were determined by gs-COSY experiments.[24]

Electrochemistry: Tetrabutylammonium hexafluorophosphate (TBAH; from Fluka), as supporting electrolyte, was used as received. Dry acetonitrile (CH_3CN), was successively heated at reflux and distilled from CaH_2 and activated alumina super I neutral (ICN Biomedicals); this was stored in a specially designed Schlenk flask over activated molecular sieves (3 Å) and protected from light. Shortly before performing the experiment, the solvent was distilled by means of a closed system into an electrochemical cell that contained the supporting electrolyte and the species under examination. Electrochemical experiments were carried out in an airtight single-compartment cell described elsewhere by using platinum and glassy carbon as working electrode, a platinum spiral as counterelectrode and a silver spiral as a quasireference electrode. The cell that contained the supporting electrolyte and the electroactive compound was dried under vacuum at about 110 °C for at least 60 h before each experiment. All the $E_{1/2}$ potentials have been directly obtained from CV curves as averages of the cathodic and anodic peak potentials for one-electron peaks and by digital simulation for those processes closely spaced in multielectron voltammetric peaks. The $E_{1/2}$ values are referenced to an aqueous saturated calomel electrode (SCE) and have been determined by adding, at the end of each experiment, ferrocene as an internal standard and measuring them with respect to the standard potential of the ferrocinium/ferrocene couple. Voltammograms were recorded with a custom-made fast potentiostat controlled with an AMEL model 568 programmable function generator. The potentiostat was interfaced with a Nicolet model 3091 digital oscilloscope and the data were transferred to a personal computer by the Antigona program.[25] The minimization of the uncompensated resistance effect in the voltammetric measurements was achieved by the positive-feedback circuit of the potentiostat.

Photophysics: Absorption spectra were measured with a Varian Cary 5000 double-beam UV/Vis/NIR spectrometer and were baseline corrected. Steady-state emission spectra were recorded with a Spex Fluorolog 1681 equipped with a 150-W xenon arc lamp, single excitation and emission monochromators and a Hamamatsu R928 photomultiplier tube or a HORIBA Jobin-Yvon IBH FL-322 Fluorolog 3 spectrometer equipped with a 450-W xenon arc lamp, double grating excitation and emission monochromators (2.1 nm mm^{-1} dispersion; 1200 grooves mm^{-1}), and a Hamamatsu R928 photomultiplier tube or a TBX-4-X single-photon-counting detector. Emission and excitation spectra were corrected for source intensity (lamp and grating) and emission spectral response (detector and grating) by standard correction curves. Time-resolved measurements were performed with: 1) Coherent Infinity Nd:YAG-XPO laser (1 ns pulses FWHM) and a Hamamatsu C5680-21 streak camera equipped with a Hamamatsu M5677 low-speed single-sweep unit; 2) the time-correlated single-photon-counting (TCSPC) option on the Fluorolog 3. NanoLEDs (295 or 402 nm; full width at half-maximum (FWHM) $<$ 750 ps) with repetition rates between 10 kHz and 1 MHz were used to excite the sample. The excitation sources were mounted directly on the sample chamber at 90° to a double-grating emission monochromator (2.1 nm mm^{-1} dispersion; 1200 grooves mm^{-1}) and collected with a TBX-4-X single-photon-counting detector. The photons collected at the detector are correlated with a time-to-amplitude converter (TAC) to the excitation pulse. Signals were collected with an IBH DataStation Hub photon-counting module and data analysis was performed using the commercially available DAS6 software (HORIBA Jobin Yvon IBH). The goodness-of-fit was assessed by minimizing the reduced chi-squared function (χ^2) and visual inspection of the weighted residuals. Luminescence quantum yields (Φ_{em}) were measured in optically dilute solutions (O.D. $<$ 0.1 at excitation wavelength) and compared to reference emitters by the following equation:[26]

$$\Phi_x = \Phi_r \left[\frac{A_r(\lambda_r)}{A_x(\lambda_x)}\right]\left[\frac{I_r(\lambda_r)}{I_x(\lambda_x)}\right]\left[\frac{n_x^2}{n_r^2}\right]\left[\frac{D_x}{D_r}\right]$$

in which A is the absorbance at the excitation wavelength (λ), I is the intensity of the excitation light at the excitation wavelength (λ), n is the refractive index of the solvent, D is the integrated intensity of the luminescence and Φ is the quantum yield. The subscripts r and x refer to the reference and the sample, respectively. All quantum yields were performed at identical excitation wavelength for the sample and the reference, thereby cancelling the $I(\lambda_r)/I(\lambda_x)$ term in the equation. All ruthenium complexes were measured against [Ru(bpy)$_3$Cl$_2$] in air-equilibrated acetonitrile as reference (Φ = 0.016). All solvents were spectrometric grade and all solutions were filtered through a 0.2 μm syringe filter before measurement. Deaerated samples were prepared by the freeze–pump–thaw technique.

Ligands Synthesis: The ligands 2-(1*H*-tetrazol-5-yl)thiophene (**2-TTH**), 5-bromo-2-(1*H*-tetrazol-5-yl)thiophene (**2-TBTH**), bis-5,5′-(1*H*-tetrazol-5-yl)-2,2′-bithiophene (**$TDTH_2$**) and bis-4,4′-(1*H*-tetrazol-5-yl)biphenyl (**$TDPH_2$**) were prepared from the corresponding nitriles by following the method reported by Mitsui and coworkers.[12d] Compound **2-TTH** (white microcrystalline powder, yield 90%): ^1H NMR ([D_6]DMSO, 400 MHz): δ = 7.26 (dd, J_1 = 3.6 Hz, J_2 = 4.8 Hz, 1 H, H-4), 7.79 (d, J = 3.6 Hz, 1 H, H-3), 7.85 (d, J = 4.8 Hz, 1 H, H-5) ppm. ^{13}C NMR ([D_6]DMSO, 100 MHz): δ = 125.4 (C_{ipso}), 128.7 (C-4), 129.3 (C-3), 130.5 (C-5), 151.4 (C_t) ppm; compound **2-TBTH** (white microcrystalline powder, 88%): ^1H NMR ([D_6]DMSO, 400 MHz): δ = 7.30 (d, J = 4.0 Hz, 1 H, H-4), 7.41 (d, J = 4.0 Hz, 1 H, H-3) ppm. ^{13}C NMR ([D_6]DMSO, 100 MHz): δ = 116.2 (C-5), 127.5 (C_{ipso}), 130.1 (C-4), 132.2 (C-3), 151.3 (C_t) ppm; **$TDTH_2$** (brown solid, 58%): ^1H NMR ([D_6]-DMSO, 400 MHz): δ = 7.61 (d, J = 4.0 Hz, 2 H, H-4), 7.78 (d, J = 4.0 Hz, 2 H, H-3) ppm. ^{13}C NMR ([D_6]DMSO, 100 MHz): δ =

 © 2010 Wiley-VCH Verlag GmbH & Co. KGaA, Weinheim

125.2 (C-5), 126.7 (C-4), 130.4 (C-3), 138.6 (C_{ipso}), 151.3 (C_t) ppm; **$TDPH_2$** ^{1}H NMR ([D$_6$]DMSO, 400 MHz): δ = 7.99 (d, J = 8.4 Hz, 2 H, H-3), 8.16 (d, J = 8.4 Hz, 2 H, H-2), 123.8 (C_{ipso}, phenyl), 127.7 (C-2), 127.8 (C-3), 141.4 (C_{ipso}, tetraz.), 155.1 (C_t) ppm.

The formation of the tetrazolate anions was achieved by addition of equimolar amounts (two equivalents in the case of the bis-tetrazolate ligands) of triethylamine to a suspension of the neutral 5-substituted tetrazoles in acetone (5 mL). The resulting colourless or pale yellow solutions were used without any further purification.

Synthesis of the Mononuclear Complexes [Ru(2-TT)][PF$_6$] and [Ru(2-TBT)][PF$_6$]: [Ru(tpy)(bpy)Cl][PF$_6$] (0.500 g, 0.74 mmol) was dissolved in deaerated acetone (15 mL) in a 100 mL Schlenk flask protected from light. A slight excess amount (1.1 equiv.) of $AgClO_4$ was added and the mixture was stirred while being heated at reflux for 2 h. The reaction mixture was cooled to r.t. and then filtered through a Celite pad. The filtrate was added dropwise to a solution of the tetrazolate ligand [**2-TT**]$^-$ (0.8 mmol) in acetone (5 mL). Once the addition was complete, the resulting solution was stirred at reflux temperature overnight. The mixture was then cooled to r.t. and concentrated to about 20 mL. Then an aqueous solution (10 mL) that contained NH_4PF_6 (around 0.5 g) was added. The resulting mixture was extracted with dichloromethane (3 × 20 mL). The organic layers were dried with $MgSO_4$ and the solvent was removed in vacuo. The solid was redissolved in a minimal quantity of dichloromethane and purified by alumina chromatography with acetone/toluene mixtures as eluent. Two bands were eluted in the following order: a purple band, identified as the starting [Ru(tpy)(bpy)Cl][PF$_6$] [acetone/toluene, 1:1 (v/v) as eluent], and a brown band, which corresponded to the target compound **[Ru(2-TT)][PF$_6$]** (acetone/toluene, 1.5:1). The fraction that contained the latter complex was evaporated to dryness, thereby affording the product as a brown powder. Crystals suitable for X-ray analysis were obtained by slow diffusion of diethyl ether into a solution of the complex in acetonitrile; yield 78%. ESI-MS: m/z = 642 [M – PF_6^-]$^+$. $C_{30}H_{22}F_6N_9PRuS$ (787.04): calcd. C 45.74, H 2.82, N 16.01; found C 45.65, H 2.90, N 15.97. ^{1}H NMR (CD_3CN, 400 MHz): δ = 6.97 (dd, J_1 = 3.6 Hz, J_2 = 5.2 Hz, 1 H, H-4L), 7.08 (t, J = 6.0 Hz, 1 H, H_i), 7.23–7.32 (m, 4 H, H-5 + H-3L + H-5), 7.45 (d, J = 5.6 Hz, 1 H, H_j), 7.75–7.81 (m, 3 H, H-6 + H_h), 7.84 (t, J = 5.6 Hz, 1 H, H_b), 7.91 (t, J = 8.0 Hz, 2 H, H-4), 8.09 (t, J = 8.0 Hz, 1 H, H-4′), 8.23 (t, J = 6.4 Hz, 1 H, H_c), 8.33 (d, J = 8.0 Hz, 2 H, H-3), 8.37 (d, J = 8.0 Hz, 1 H, H_g), 8.42 (d, J = 8.0 Hz, 2 H, H-3′), 8.61 (d, J = 8.0 Hz, 1 H, H_d), 9.47 (d, J = 5.6 Hz, 1 H, H_a) ppm. ^{13}C NMR (CD_3CN, 400 MHz): δ = 123.5 (C-3′), 124.2 (C_g), 124.5 (C-3), 124.7 (C_d), 125.7 (C-5L), 126.5 (C-3L), 127.2 (C_i), 128.0 (C_b), 128.3 (C-5), 128.5 (C-4L), 132.6 (C_{ipso}-t), 135.9 (C-4′), 137.5 (C_h), 137.8 (C_c), 138.5 (C-4), 152.4 (C_j), 153.7 (C_a), 153.8 (C-6), 157.1 (C_e), 158.5 (C_f), 158.9 (C_t), 159.1 (C-2′), 159.7 (C-2) ppm.

Compound **[Ru(2-TBT)][PF$_6$]** was prepared according to the same procedure described for **[Ru(2-TT)][PF$_6$]**, by treating [Ru(tpy)(bpy)Cl][PF$_6$] (0.500 g, 0.74 mmol) with [**2-TBT**]$^-$ (0.8 mmol). The crude product was purified by alumina chromatography with acetone/toluene mixtures as eluent. Two bands were eluted in the following order: a brown band, which corresponded to the target product **[Ru(2-TBT)][PF$_6$]** (acetone/toluene, 1:1.5 as eluent), and a purple band, identified as the starting [Ru(tpy)(bpy)Cl][PF$_6$] (acetone/toluene, 1:1). The fraction that contained the former complex was evaporated to dryness, thereby affording the product as a brown microcrystalline powder. Crystals suitable for X-ray analysis were obtained by slow diffusion of diethyl ether into a solution of the complex in acetonitrile; yield 85%. ESI-MS: m/z = 720, 722 [M – PF_6^-]$^+$. $C_{30}H_{21}BrF_6N_9PRuS$ (864.95): calcd. C 41.62, H 2.45, N 14.57; found C 41.75, H 2.39, N 14.63. ^{1}H NMR (CD_3CN, 400 MHz): δ = 6.98 (d, J = 4.0 Hz, 1 H, H-4L), 7.03 (d, J = 4.0 Hz, 1 H, H-3L), 7.07 (t, J = 6.0 Hz, 1 H, H_i), 7.28 (t, J = 6.4 Hz, 2 H, H-5), 7.44 (d, J = 5.6 Hz, 1 H, H_j), 7.75–7.84 (m, 4 H, H-6 + H_h + H_b), 7.88 (t, J = 8.0 Hz, 2 H, H-4), 8.06 (t, J = 8.0 Hz, 1 H, H-4′), 8.23 (t, J = 6.4 Hz, 1 H, H_c), 8.30 (d, J = 8.0 Hz, 2 H, H-3), 8.37 (d, J = 8.0 Hz, 1 H, H_g), 8.39 (d, J = 8.0 Hz, 2 H, H-3′), 8.61 (d, J = 8.0 Hz, 1 H, H_d), 9.43 (d, J = 5.6 Hz, 1 H, H_a) ppm. ^{13}C NMR (CD_3CN, 400 MHz): δ = 112.5 (C-5L), 123.5 (C-3′), 124.2 (C_g), 124.5 (C-3), 125.1 (C_d), 125.9 (C-3L), 127.3 (C_i), 128.0 (C_b), 128.3 (C-5), 131.1 (C-4L), 134.7 (C_{ipso}-t), 135.9 (C-4′), 137.5 (C_h), 137.8 (C_c), 138.5 (C-4), 152.3 (C_j), 153.6 (C_a), 153.8 (C-6), 157.1 (C_e), 158.5 (C_f), 159.0 (C-2′), 159.6 (C-2), 159.8 (C_t) ppm.

Methylation Reaction: [Ru(2-TT)][PF$_6$] (0.100 g, 0.127 mmol) was dissolved in dichloromethane (10 mL) and the resulting brown solution was cooled to –50 °C; then $CH_3SO_3CF_3$ (2.55 mL, 0.05 M in dichloromethane; 0.127 mmol) was added dropwise. After 30 min, the red-orange mixture was warmed to r.t. and stirred for an additional 4 h. Evaporation of the solvent afforded a red-orange solid that was dissolved into a minimal amount of acetonitrile. Then an aqueous solution (10 mL) that contained NH_4PF_6 (around 0.5 g) was added. The resulting mixture was extracted with dichloromethane (3 × 20 mL). The organic layers were dried with $MgSO_4$ and the solvent was removed in vacuo, thereby affording a red-orange solid, which was identified as the methylated product **[Ru{2-(Me)TT}][PF$_6$]$_2$**. Crystals suitable for X-ray analysis were obtained by slow diffusion of diethyl ether into a solution of the complex in acetonitrile; yield 91%. ESI-MS: m/z = 329 [M – $2PF_6^-$]$^{2+}$. $C_{31}H_{25}F_{12}N_9P_2RuS$ (947.03): calcd. C 39.28, H 2.66, N 13.31; found C 39.40, H 2.57, N 13.41. ^{1}H NMR (CD_3CN, 400 MHz): δ = 3.91 (s, 3 H, Me), 7.14 (t, J = 6.8 Hz, 1 H, H_i), 7.18 (dd, J_1 = 4.0, J_2 = 4.8 Hz, 1 H, H-4L), 7.35 (t, J = 6.4 Hz, 2 H, H-5), 7.46 (d, J = 5.2 Hz, 1 H, H_j), 7.53 (d, J = 4.0 Hz, 1 H, H-3L), 7.72 (d, J = 4.8 Hz, 1 H, H-5), 7.79–7.90 (m, 4 H, H-6 + H_h + H_b), 7.98 (t, J = 8.0 Hz, 2 H, H-4), 8.22 (t, J = 8.0 Hz, 1 H, H-4′), 8.28–8.44 (m, 4 H, H-3 + H_c + H_g), 8.50 (d, J = 8.0 Hz, 2 H, H-3′), 8.66 (d, J = 8.0 Hz, 1 H, H_d), 9.30 (d, J = 5.2 Hz, 1 H, H_a) ppm. ^{13}C NMR (CD_3CN, 400 MHz): δ = 36.9 (Me), 121.3 (C_{ipso}-t), 124.2 (C-3′), 124.4 (C_g), 124.9 (C-3), 125.1 (C_d), 127.6 (C_i), 128.2 (C_b), 128.7 (C-5), 129.8 (C-4L), 132.4 (C-3L), 133.1 (C-5L), 137.5 (C-4′), 138.3 (C_h), 138.5 (C_c), 139.3 (C-4), 152.0 (C_t), 152.4 (C_j), 153.3 (C_a), 154.1 (C-6), 157.1 (C_e), 158.4 (C_f), 159.0 (C-2′), 159.7 (C-2) ppm.

Compound **[Ru{2-(Me)TBT}][PF$_6$]$_2$** was prepared according to the same procedure described for **[Ru{2-(Me)TT}][PF$_6$]$_2$**, by treating **[Ru(2-TBT)][PF$_6$]** (0.100 g, 0.116 mmol) with $CH_3SO_3CF_3$ (2.30 mL, 0.05 M in dichloromethane; 0.116 mmol). The target product **[Ru{2-(Me)TBT}][PF$_6$]$_2$** was obtained as a red solid; yield 87%. $C_{31}H_{24}BrF_{12}N_9P_2RuS$ (1024.94): calcd. C 36.29, H 2.36, N 12.30; found C 36.18, H 2.50, N 12.35. ^{1}H NMR (CD_3CN, 400 MHz): δ = 3.91 (s, 3 H, Me), 7.13 (t, J = 6.8 Hz, 1 H, H_i), 7.21 (d, J = 4.0 Hz, 1 H, H-4L), 7.35 (t, J = 6.4 Hz, 2 H, H-5), 7.41–7.43 (m, 2 H, H_j + H-3L), 7.74 (d, J = 5.2 Hz, 2 H, H-6), 7.81–7.90 (m, 2 H, H_h + H_b), 7.98 (t, J = 7.6 Hz, 2 H, H-4), 8.24 (t, J = 8.0 Hz, 1 H, H-4′), 8.30 (t, J = 7.6 Hz, 1 H, H_c), 8.66–8.72 (m, 3 H, H-3 + H_g), 8.83 (d, J = 8.0 Hz, 2 H, H-3′), 8.92 (d, J = 8.0 Hz, 1 H, H_d), 9.25 (d, J = 5.2 Hz, 1 H, H_a) ppm. ^{13}C NMR (CD_3CN, 400 MHz): δ = 37.0 (Me), 118.7 (C-5L), 124.0 (C_{ipso}-t), 124.6 (C-3′), 124.8 (C_g), 125.4 (C-3), 125.5 (C_d), 127.5 (C_i), 128.2 (C_b), 128.6 (C-5), 133.0 (C-4L), 133.1 (C-3L), 137.6 (C-4′), 138.2 (C_h), 138.5 (C_c), 139.3 (C-4), 152.0 (C_t), 152.1 (C_j), 153.2 (C_a), 153.8 (C-6), 157.0 (C_e), 158.3 (C_f), 158.7 (C-2′), 159.6 (C-2) ppm.

Protonation Reaction: [Ru(2-TT)][PF$_6$] (0.100 g, 0.127 mmol) was dissolved in dichloromethane (10 mL) and the resulting brown

 © 2010 Wiley-VCH Verlag GmbH & Co. KGaA, Weinheim

solution was cooled to –50 °C; then HSO_3CF_3 (2.55 mL, 0.05 M in dichloromethane; 0.127 mmol) was added dropwise. After 30 min, the red-orange mixture was warmed to r.t. and stirred for an additional hour. Evaporation of the solvent afforded, almost quantitatively, an orange solid that corresponded to the protonated product **[Ru{2-(H)TT}][SO_3CF_3]$_2$**. Crystals suitable for X ray analysis were obtained by slow diffusion of diethyl ether into a solution of the complex in acetonitrile. $C_{32}H_{23}F_6N_9O_6RuS_3$ (940.99): calcd. C 40.81, H 2.46, N 13.39; found C 40.69, H 2.50, N 13.49. ^{1}H NMR (CD_3CN, 400 MHz): δ = 7.11–7.18 (m, 2 H, H-4L + H_i), 7.35 (t, J = 6.4 Hz, 2 H, H-5), 7.45 (d, J = 5.2 Hz, 1 H, H_j), 7.65–7.71 (m, 2 H, H-3L + H-5), 7.80–7.87 (m, 4 H, H-6 + H_h + H_b), 7.98 (t, J = 8.0 Hz, 2 H, H-4), 8.21 (t, J = 8.0 Hz, 1 H, H-4′), 8.29 (t, J = 8.0 Hz, 1 H, H_c), 8.40–8.46 (m, 3 H, H-3 + H_g), 8.52 (d, J = 8.0 Hz, 2 H, H-3′), 8.69 (d, J = 8.0 Hz, 1 H, H_d), 9.23 (d, J = 5.2 Hz, 1 H, H_a) ppm. ^{13}C NMR (CD_3CN, 400 MHz): δ = 123.3 ($C_{ipso\text{-}t}$), 124.2 (C-3′), 124.4 (C_g), 124.9 (C-3), 125.1 (C_d), 127.6 (C_i), 128.2 (C_b), 128.6 (C-5), 129.7 (C-4L), 131.5 (C-3L), 132.6 (C-5L), 137.4 (C-4′), 138.2 (C_h), 138.4 (C_c), 139.3 (C-4), 152.3 (C_j), 152.7 (C_t), 153.3 (C_a), 154.1 (C-6), 157.1 (C_e), 158.4 (C_f), 158.9 (C-2′), 159.6 (C-2) ppm.

Synthesis of the Dinuclear Complexes [Ru(TDT)Ru][PF_6]$_2$ and [Ru(TDP)Ru][BF_4]$_2$: [Ru(tpy)(bpy)Cl][PF_6] (0.764 g, 1.14 mmol) was dissolved in an acetone/water mixture (15 mL, 3:1 v/v) in a 100 mL Schlenk protected from light. A slight excess amount (1.1 equiv.) of $AgPF_6$ was added and the mixture was stirred while being heated to reflux for 3 h. The reaction mixture was cooled to r.t., then filtered through a Celite pad, and the filtrate was added dropwise to a solution of the tetrazolate ligand [**TDT**]$^-$ (0.5 mmol) in acetone (10 mL) . Once the addition was complete, the resulting solution was stirred at reflux temperature overnight. The mixture was then cooled to r.t. and concentrated to about 20 mL. Then an aqueous solution (10 mL) that contained NH_4PF_6 (around 0.5 g) was added. The resulting mixture was extracted with dichloromethane (3 × 20 mL). The organic layers were dried with $MgSO_4$ and the solvent was removed in vacuo. The solid was redissolved in a minimal quantity of dichloromethane and purified by alumina chromatography with acetone/toluene mixtures as eluent. The target product **[Ru(TDT)Ru][PF_6]$_2$** was eluted with an acetone/toluene mixture, 3:1 (v/v); yield 17%. ESI-MS: m/z = 641 [M – 2PF_6^-]$^{2+}$. $C_{60}H_{42}F_{12}N_{18}P_2Ru_2S_2$ (1572.07): calcd. C 45.80, H 2.69, N 16.03; found C 45.65, H 2.80, N 15.97. ^{1}H NMR (CD_3CN, 400 MHz): δ = 7.04 (d, J = 3.6 Hz, 2 H, H-4L), 7.06 (t, J = 8.0 Hz, 2 H, H_b), 7.14 (d, J = 3.6 Hz, 2 H, H-3L), 7.27 (t, J = 6.0 Hz, 4 H, H-5), 7.44 (d, J = 5.2 Hz, 2 H, H_a), 7.74–7.86 (m, 8 H, H-6 + H_c + H_i), 7.88 (t, J = 7.2 Hz, 4 H, H-4), 8.05 (t, J = 8.0 Hz, 2 H, H-4′), 8.22 (t, J = 7.2 Hz, 2 H, H_h), 8.30 (d, J = 4.0 Hz, 4 H, H-3), 8.35–8.40 (m, 6 H, H-3′ + H_d), 8.60 (d, J = 4.0 Hz, 2 H, H_g), 9.46 (d, J = 5.2 Hz, 2 H, H_j) ppm. ^{13}C NMR (CD_3CN, 400 MHz): δ = 123.5 (C-5), 124.1 (C_i), 124.4 (C-3′), 124.6 (C_g), 125.1 (C-3L), 126.4 (C-4L), 127.2 (C_b), 127.9 (C_d), 128.2 (C-3), 132.4 (C-5L), 135.8 (C-4′), 137.3 ($C_{ipso\text{-}t}$), 137.4 (C_h), 137.7 (C_c), 138.4 (C-4), 152.3 (C_j), 153.5 (C_a), 153.6 (C-6), 157.0 (C_f), 158.4 (C_e), 159.0 (C-2′), 159.6 (C-2), 160.1 (C_t) ppm.

Compound **[Ru(TDP)Ru][BF_4]$_2$** was prepared by the same procedure described for [Ru(TDT)Ru][PF_6]$_2$, by treating [Ru(tpy)(bpy)Cl][PF_6] (0.5 mmol) with $AgBF_4$ (1.1 equiv.), and then with [**TDP**]$^-$ (0.27 mmol). The crude product was purified by alumina chromatography with acetone/toluene mixtures as eluent. The target product **[Ru(TDP)Ru][BF_4]$_2$** was eluted with an acetone/toluene mixture, 3:1 (v/v); yield 32%. ESI-MS: m/z = 635 [M – 2BF_4^-]$^{2+}$. $C_{64}H_{46}B_2F_8N_{18}Ru_2$ (1444.23): calcd. C 53.18, H 3.21, N 17.45; found C 53.05, H 3.28, N 17.51. ^{1}H NMR (CD_3CN, 400 MHz): δ = 7.08 (t, J = 5.7 Hz, 2 H, H_b), 7.29 (t, J = 7.2 Hz, 4 H, H-5), 7.46 (d, J = 6.3 Hz, 2 H, H_a), 7.56 (d, J = 6.9 Hz, 4 H, H_L), 7.76 (d, J = 6.9 Hz, 4 H, H_L), 7.80–7.93 (m, 8 H, H-6 + H_c + H_i), 8.08 (t, J = 4.8 Hz, 2 H, H-4), 8.23 (t, J = 4.8 Hz, 2 H, H-4′), 8.31 (t, J = 7.8 Hz, 2 H, H_h), 8.34 (d, J = 5.4 Hz, 4 H, H-3), 8.34–8.41 (m, 6 H, H-3′ + H_d), 8.62 (d, J = 8.1 Hz, 2 H, H_g), 9.51 (d, J = 5.7 Hz, 2 H, H_j) ppm. ^{13}C NMR (CD_3CN, 400 MHz): δ = 123.5 (C-5), 124.1 (C_i), 124.4 (C-3′), 124.6 (C_g), 127.2 (C_b), 127.2 (C-3L), 127.7 (C-4L), 127.9 (C_d), 128.2 (C-3), 130.4 (C-5L), 135.7 (C-4′), 137.4 (C_c), 137.7 (C-4), 138.4 (C_h), 140.9 ($C_{ipso\text{-}t}$), 152.3 (C_j and C_a) 153.7 (C-6), 157.0 (C_f), 158.5 (C_e), 159.0 (C-2′), 159.6 (C-2), 164.2 (C_t) ppm.

Methylation Reaction: [Ru(TDT)Ru][PF_6]$_2$ (0.060 g, 0.038 mmol) was dissolved in acetonitrile (10 mL) and the resulting solution was cooled to –50 °C; then $CH_3SO_3CF_3$ (1.6 mL, 0.05 M in dichloromethane; 0.08 mmol) was added dropwise. After 1 h, the resulting solution was warmed to r.t. and stirred for additional 2 h. Then an aqueous solution (10 mL) that contained NH_4PF_6 (around 0.5 g) was added. The resulting mixture was extracted with dichloromethane (3 × 20 mL). The organic layers were dried with $MgSO_4$ and the solvent was removed in vacuo to afford, almost quantitatively, the methylated product **[Ru(Me)(TDT)(Me)Ru][PF_6]$_4$**. $C_{62}H_{48}F_{24}N_{18}P_4Ru_2S_2$ (1892.04): calcd. C 39.32, H 2.56, N 13.32; found C 39.18, H 2.68, N 13.19. ^{1}H NMR (CD_3CN, 400 MHz): δ = 3.48 (s, 6 H, Me), 7.26 (t, J = 6.0 Hz, 2 H, H_b), 7.45 (d, J = 4.0 Hz, 2 H, H-4L), 7.49 (t, J = 6.4 Hz, 4 H, H-5), 7.61 (d, J = 4.0 Hz, 2 H, H-3L), 7.71 (d, J = 5.6 Hz, 2 H, H_a), 7.92–7.96 (m, 4 H, H_c + H_i), 8.02 (d, J = 4.8 Hz, 4 H, H-6), 8.09 (t, J = 8.0 Hz, 4 H, H-4), 8.30 (t, J = 8.0 Hz, 2 H, H-4′), 8.37 (t, J = 8.0 Hz, 2 H, H_h), 8.59–8.65 (m, 6 H, H-3′ + H_d), 8.70 (d, J = 8.4 Hz, 4 H, H-3), 8.86 (d, J = 8.4 Hz, 2 H, H_g), 9.42 (d, J = 6.0 Hz, 2 H, H_j) ppm. ^{13}C NMR (CD_3CN, 400 MHz): δ = 34.8 (Me), 121.2 (C-5L), 122.1 (C-5), 122.3 (C_i), 122.4 (C_g), 122.8 (C-3′), 125.6 (C_b), 126.3 (C-4L), 126.7 (C-3), 131.2 (C-3L), 135.6 (C-4′), 136.2 (C_h), 136.4 (C_c), 137.2 (C-4), 139.0 ($C_{ipso\text{-}t}$), 150.1 (C_j), 150.3 (C_t), 151.2 (C_a), 151.9 (C-6), 154.8 (C_f), 156.3 (C_e), 156.7 (C-2′), 157.5 (C-2) ppm.

Compound **[Ru(Me)(TDP)(Me)Ru][PF_6]$_4$** was prepared according to the same procedure described for **[Ru(Me)(TDT)(Me)Ru][PF_6]$_4$** by treating **[Ru(TDP)Ru][BF_4]$_2$** (0.060 g, 0.042 mmol) with $CH_3SO_3CF_3$ (1.8 mL, 0.05 M in dichloromethane; 0.09 mmol). $C_{66}H_{52}F_{24}N_{18}P_4Ru_2$ (1880.13): calcd. C 42.12, H 2.79, N 13.41; found C 42.01, H 2.68, N 13.58. ^{1}H NMR (CD_3CN, 400 MHz): δ = 7.14 (t, J = 3.2 Hz, 2 H, H_b), 7.36 (t, J = 8.8 Hz, 4 H, H-5), 7.46 (d, J = 5.2 Hz, 2 H, H_a), 7.58 (d, J = 6.9 Hz, 4 H, H_L), 7.79 (d, J = 6.9 Hz, 4 H, H_L), 7.82–7.91 (m, 8 H, H-6 + H_c + H_i), 7.98 (t, J = 8.0 Hz, 4 H, H-4), 8.25 (t, J = 4.0 Hz, 2 H, H-4′), 8.33 (t, J = 6.0 Hz, 2 H, H_h), 8.39–8.44 (m, 6 H, H_d + H-5), 8.52 (d, J = 8.4 Hz, 4 H, H-3′), 8.67 (d, J = 8.0 Hz, 2 H, H_g), 9.34 (d, J = 2 H, H_j, 4.8 Hz) ppm. ^{13}C NMR (CD_3CN, 400 MHz): δ = 36.9 (Me), 118.3 (C-5L), 124.2 (C-5), 124.4 (C_i), 124.9 (C-3′), 125.1 (C_g), 127.6 (C_b), 128.2 (C_d), 128.6 (C-3), 128.9 (C-4L), 130.3 (C-3L), 137.4 (C-4′), 138.2 (C_h), 138.4 (C_c), 139.3 (C-4), 143.5 ($C_{ipso\text{-}t}$), 152.3 (C_j and C_a), 153.3 (C_t), 154.1 (C-6), 157.2 (C_f)158.3 (C_e), 158.9 (C-2′), 159.6 (C-2) ppm.

X-ray Crystallography: Crystal data and collection details are reported in Table 5. The diffraction experiments were carried out with a Bruker APEX II diffractometer (for **[Ru(2-TBT)][PF_6]·2CH_3CN**) and with a Bruker SMART 2000 diffractometer {for **[Ru(2-TT)][PF_6]**, **[Ru{2-(H)TT}][CF_3SO_3]$_2$·CH_3CN** and **[Ru{2-(Me)TT}][PF_6]$_2$·2CH_3CN**} equipped with a CCD detector and using Mo-K_α radiation. Data were corrected for Lorentz polarization and absorption effects (empirical absorption correction SAD-

 © 2010 Wiley-VCH Verlag GmbH & Co. KGaA, Weinheim

Table 5. Crystal data and collection details for **[Ru(2-TT)][PF_6]**, **[Ru(2-TBT)][PF_6]·2CH_3CN**, **[Ru{2-(H)TT}][CF_3SO_3]$_2$·CH_3CN** and **[Ru{2-(Me)TT}][PF_6]$_2$·2CH_3CN**.

		[Ru(2-TBT)][PF_6]·2CH_3CN	[Ru{2-(H)TT}][CF_3SO_3]$_2$·CH_3CN	[Ru{2-(Me)TT}][PF_6]$_2$·2CH_3CN
Formula	$C_{30}H_{22}F_6N_9PRuS$	$C_{34}H_{27}BrF_6N_{11}PRuS$	$C_{34}H_{26}F_6N_{10}O_6RuS_3$	$C_{35}H_{31}F_{12}N_{11}P_2RuS$
M_r	786.67	847.68	981.90	1028.78
T [K]	293(2)	296(2)	293(2)	293(2)
λ [Å]	0.71073	0.71073	0.71073	0.71073
Crystal system	triclinic	triclinic	monoclinic	monoclinic
Space group	$P\bar{1}$	$P\bar{1}$	$P2_1$	Pc
a [Å]	8.7899(18)	8.8097(5)	10.892(2)	8.9526(18)
b [Å]	12.802(3)	12.7092(8)	9.3322(19)	10.902(2)
c [Å]	14.609(3)	18.4351(11)	20.681(5)	22.008(4)
α [°]	71.45(13)	103.5080(10)	90	90
β [°]	76.58(3)	102.8710(10)	104.04(3)	96.43(3)
γ [°]	77.06(3)	100.3610(10)	90	90
Cell volume [Å^3]	1495.7(5)	1897.1(2)	2039.4(7)	2134.5(7)
Z	2	2	2	2
D_c [gcm^{-3}]	1.747	1.659	1.599	1.601
μ [mm^{-1}]	0.726	1.636	0.622	0.585
F(000)	788	944	988	1032
Crystal size [mm]	0.19×0.16×0.11	0.22×0.16×0.12	0.32×0.25×0.19	0.24×0.20×0.12
θ limits [°]	1.49–25.03	1.70–25.68	1.01–28.70	1.86–30.51
Index ranges	$-10 \le h \le 10$	$-10 \le h \le 10$	$-14 \le h \le 14$	$-12 \le h \le 12$
	$-15 \le k \le 15$	$-15 \le k \le 15$	$-12 \le k \le 12$	$-15 \le k \le 15$
	$-17 \le l \le 17$	$-22 \le l \le 22$	$-27 \le l \le 27$	$-31 \le l \le 31$
Reflections collected	13333	19491	24325	28399
Independent reflections	5291 (R_{int} = 0.0613)	7188 (R_{int} = 0.0254)	10450 (R_{int} = 0.0319)	12896 (R_{int} = 0.0523)
Completeness to θ max. [%]	100.0	99.6	100.0	100.0
Data/restraints/parameters	5291/0/433	7188/0/5015	10450/2/530	12896/215/533
Goodness-of-fit on F^2	1.045	1.072	1.051	1.001
$R1$ [$I>2\sigma(I)$]	0.0471	0.0415	0.0396	0.0575
$wR2$ (all data)	0.1218	0.1307	0.1107	0.1567
Absolute structure parameter	–	–	0.04(2)	0.48(6)
Largest diff. peak and hole [e Å^{-3}]	0.646/–0.574	1.185/–0.758	0.805/–0.449	0.741/–0.384

ABS).[27] Structures were solved by direct methods and refined by full-matrix least-squares on the basis of all data using F^2.[28] Hydrogen atoms were placed in calculated positions, except for H(90) in **[Ru{2-(H)TT}][CF_3SO_3]$_2$·CH_3CN**, which was located in the Fourier map and refined with the N(9)–H(90) distance restrained to 0.86 Å (standard uncertainty: 0.02). Hydrogen atoms were treated isotropically by using the 1.2-fold U_{iso} value of the parent atom, except for methyl protons, which were assigned the 1.5-fold U_{iso} value of the parent C atom. All non-hydrogen atoms were refined with anisotropic displacement parameters. The crystals of **[Ru{2-(Me)TT}][PF_6]$_2$·2CH_3CN** appeared to be racemically twinned with a refined Flack parameter of 0.48(6).[29]

CCDC-761566 (for **[Ru(2-TBT)]$^+$**), -761567 (for **[Ru{2-(H)-TT}]$^{2+}$**), -761568 (for **[Ru{2-(Me)TT}]$^{2+}$**) and -761569 (for **[Ru(2-TT)]$^+$**) contain the supplementary crystallographic data for this paper. These data can be obtained free of charge from The Cambridge Crystallographic Data Centre via www.ccdc.cam.ac.uk/data_request/cif.

Supporting Information (see also the footnote on the first page of this article): Selected ^{1}H and ^{13}C NMR, absorption, emission and excitation (77 K) spectra of the complexes together with the cyclic voltammogram of **[Ru(TDT)Ru]$^{2+}$**.

Acknowledgments

The authors wish to thank the Italian Ministero per l'Istruzione, Università a Ricerca and theUniversity of Bologna for financial support.

[1] a) S. Campagna, F. Puntoriero, F. Nastasi, G. Bergamini, V. Balzani, *Top. Curr. Chem.* **2007**, *280*, 117–214; b) H. Hofmeier, U. S. Schubert, *Chem. Soc. Rev.* **2004**, *33*, 373; c) J. P. Sauvage, J. P. Collin, J. C. Chambron, S. Guillerez, C. Coudret, V. Balzani, F. Barigelletti, L. De Cola, L. Flamigni, *Chem. Rev.* **1994**, *94*, 993; d) V. Balzani, F. Scandola, *Supramolecular Photochemistry*, Ellis Horwood, Chichester, U.K., **1991**.

[2] J. G. Vos, J. M. Kelly, *Dalton Trans.* **2006**, 4869–4883 and references cited therein.

[3] For sunlight-driven water-splitting systems, see: a) D. Gust, T. A. Moore, A. L. Moore, *Acc. Chem. Res.* **2009**, *42*, 1890–1898; b) A. Magnuson, M. Anderlund, O. Johansson, P. Lindblad, R. Lomoth, T. Polivka, S. Ott, K. Stensjö, S. Styring, V. Sundström, L. Hammarström, *Acc. Chem. Res.* **2009**, *42*, 1899–1909; c) J. J. Concepcion, J. W. Jurss, M. K. Brennaman, P. G. Hoertz, A. O. T. Patrocinio, N. Y. M. Iha, J. L. Templeton, T. J. Meyer, *Acc. Chem. Res.* **2009**, *42*, 1954–1965, and references cited therein; for Ru-based DSSC systems, see: d) A. Mishra, N. Pootrakulchote, M. K. R. Fischer, C. Klein, M. K. Nazeeruddin, S. M. Zakeeruddin, P. Baüerle, M. Grätzel, *Chem. Commun.* **2009**, 7146–7148 and references cited therein; e) M. K. Nazeeruddin, F. De Angelis, S. Fantacci, A. Selloni, G. Viscardi, P. Liska, S. Ito, T. Bessho, M. Grätzel, *J. Am. Chem. Soc.* **2005**, *127*, 16835–16847; see also: f) W. J. Youngblood, S.-H. A. Lee, K. Maeda, T. E. Mallouk, *Acc. Chem. Res.* **2009**, *42*, 1966–1973 and references cited therein.

[4] For some reviews, see: a) W. J. Miao, *Chem. Rev.* **2008**, *108*, 2506–2553; b) M. M. Richter, *Chem. Rev.* **2004**, *104*, 3003–3036; c) C.-Y. Liu, A. J. Bard, *Acc. Chem. Res.* **1999**, *32*, 235–245; see also: d) S. Weller, K. Brunner, J. W. Hofstraat, L. De Cola, *Nature* **2003**, *421*, 54–57.

 © 2010 Wiley-VCH Verlag GmbH & Co. KGaA, Weinheim

[5] a) C. A. Puckett, J. K. Barton, *J. Am. Chem. Soc.* **2009**, *131*, 8738–8739, and references cited therein; b) R. Blasius, H. Nierengarten, M. Luhmer, J. F. Constant, E. Defrancq, P. Dumy, A. van Dorsselaer, C. Moucheron, A. Kirsch-De Mesmaeker, *Chem. Eur. J.* **2005**, *11*, 1507–1517; c) K. E. Erkkila, D. T. Odom, J. K. Barton, *Chem. Rev.* **1999**, *99*, 2777–2795.

[6] For a review, see: M. Wang, Y. Na, M. Gorlov, L. Sun, *Dalton Trans.* **2009**, 6458–6467; see also: S. Rau, D. Walther, J. G. Vos, *Dalton Trans.* **2007**, 915–919; H. Ozawa, M. Haga, K. Sakai, *J. Am. Chem. Soc.* **2006**, *128*, 4926–4927; S. Rau, B. Schäfer, D. Gleich, E. Anders, M. Rudolph, M. Friedrich, H. Görls, W. Henry, J. G. Vos, *Angew. Chem. Int. Ed.* **2006**, *45*, 6215–6218.

[7] a) S. Stagni, E. Orselli, A. Palazzi, L. De Cola, S. Zacchini, C. Femoni, M. Marcaccio, F. Paolucci, S. Zanarini, *Inorg. Chem.* **2007**, *46*, 9126–9138; b) S. Stagni, A. Palazzi, S. Zacchini, B. Ballarin, C. Bruno, M. Marcaccio, F. Paolucci, M. Monari, M. Carano, A. J. Bard, *Inorg. Chem.* **2006**, *45*, 695–709; c) M. Massi, M. Cavallini, S. Stagni, A. Palazzi, F. Biscarini, *Mater. Sci. Eng. C* **2003**, *23*, 923–925; d) M. Duati, S. Tasca, F. C. Lynch, H. Bohlen, J. G. Vos, S. Stagni, M. D. Ward, *Inorg. Chem.* **2003**, *42*, 8377–8384.

[8] A. J. Downard, P. J. Steel, J. Steenwijk, *Aust. J. Chem.* **1995**, *48*, 1625–1642.

[9] a) I. F. Perepichka, D. F. Perepichka (Eds.), *Handbook of Thiophene Based Materials: Applications in Organic Electronics and Photonics*, Wiley, Hoboken, New Jersey, **2009**; b) A. Mishra, C.-Q. Ma, P. Bäuerle, *Chem. Rev.* **2009**, *109*, 1141–1276, and references therein; see also: c) S. Karpe, M. Ocafran, K. Smaali, S. Lenfant, D. Vuillaume, P. Blanchard, J. Roncali, *Chem. Commun.* **2010**, *46*, 3657; d) M. Melucci, L. Favaretto, C. Bettini, M. Gazzano, N. Camaioni, P. Maccagnani, P. Ostoja, M. Monari, G. Barbarella, *Chem. Eur. J.* **2007**, *13*, 10046–10054; e) G. Barbarella, M. Melucci, G. Sotgiu, *Adv. Mater.* **2005**, *17*, 1581–1593.

[10] a) A. Belbakra, S. Goeb, A. De Nicola, R. Ziessel, C. Sabatini, A. Barbieri, F. Barigelletti, *Inorg. Chem.* **2007**, *46*, 839–847, and references therein; b) A. Harriman, G. Izzet, S. Goeb, A. De Nicola, R. Ziessel, *Inorg. Chem.* **2006**, *45*, 9729–9741; c) A. Barbieri, B. Ventura, L. Flamigni, F. Barigelletti, G. Fuhrmann, P. Bäuerle, S. Goeb, R. Ziessel, *Inorg. Chem.* **2005**, *44*, 8033–8043; d) R. Ziessel, P. Bäuerle, M. Ammann, A. Barbieri, F. Barigelletti, *Chem. Commun.* **2005**, 802–804; e) J. Hjelm, E. C. Constable, E. Figgermeier, A. Hagfeldt, R. Handel, C. E. Housecroft, E. Mukhtar, E. Schofield, *Chem. Commun.* **2002**, 284–285.

[11] a) C.-H. Chen, M. Wang, J.-Y. Li, N. Pootrakulchote, L. Alibabaei, C. Ngoc-le, J.-D. Decoppet, C. Grätzel, C.-G. Wu, S. M. Zakeeruddin, M. Grätzel, *ACS Nano* **2009**, *3*, 3103–3109; b) J.-J. Kim, H. Choi, C. Kim, M.-S. Kang, J. Ko, *Chem. Mater.* **2009**, *21*, 5719–5726, and references cited therein.

[12] a) R. N. Butler, *Comprehensive Heterocyclic Chemistry II* (Ed.: R. C. Storr), vol. 4, Pergamon Press, Oxford, U.K., **1996**, pp. 621–678; b) V. Auleggi, G. Sedelmeier, *Angew. Chem. Int. Ed.* **2007**, *46*, 8440–8444; c) Z. P. Demko, K. B. Sharpless, *J. Org. Chem.* **2001**, *66*, 7945–7950; d) K. Koguro, T. Oga, S. Mitsui, R. Orita, *Synthesis* **1998**, 910–915; e) W. G. Finnegan, R. A. Henry, R. Lofquist, *J. Am. Chem. Soc.* **1958**, *80*, 3908–3911.

[13] M. Kuroboshi, Y. Waki, H. Tanaka, *J. Org. Chem.* **2003**, *68*, 3938–3942.

[14] S. C. Rasmussen, S. E. Ronco, D. A. Mlsna, M. A. Billadeau, W. T. Pennington, J. W. Kolis, J. D. Petersen, *Inorg. Chem.* **1995**, *34*, 821–829.

[15] C. Di Pietro, S. Serroni, S. Campagna, T. Gandolfi, R. Ballardini, S. Fanni, W. R. Browne, J. G. Vos, *Inorg. Chem.* **2002**, *41*, 2871–2878.

[16] a) A. Palazzi, S. Stagni, *J. Organomet. Chem.* **2005**, *690*, 2052–2061; b) A. Palazzi, S. Stagni, M. Monari, S. Selva, *J. Organomet. Chem.* **2003**, *669*, 135–140; c) A. Palazzi, S. Stagni, S. Bordoni, M. Monari, S. Selva, *Organometallics* **2002**, *21*, 3774–3781.

[17] a) X.-J. Yang, F. Drepper, B. Wu, W.-H. Sun, W. Haehnel, C. Janiak, *Dalton Trans.* **2005**, 256–267; b) E. Sondaz, J. Jaud, J. P. Launay, J. Bonvoisin, *Eur. J. Inorg. Chem.* **2002**, 1924–1927; c) E. Sondaz, A. Gourdon, J. P. Launay, J. Bonvoisin, *Inorg. Chim. Acta* **2001**, *316*, 79–88.

[18] a) V. Balzani, A. Juris, M. Venturi, S. Campagna, S. Serroni, *Acc. Chem. Res.* **1998**, *31*, 26 and references therein; b) M. Marcaccio, F. Paolucci, C. Paradisi, S. Roffia, C. Fontanesi, L. J. Yellowlees, S. Serroni, S. Campagna, V. Balzani, *J. Am. Chem. Soc.* **1999**, *121*, 10081; c) M. Marcaccio, F. Paolucci, C. Paradisi, M. Carano, S. Roffia, C. Fontanesi, L. J. Yellowlees, S. Serroni, S. Campagna, V. Balzani, *J. Electroanal. Chem.* **2002**, *532*, 99; d) M. Marcaccio, F. Paolucci, C. Fontanesi, G. Fioravanti, S. Zanarini, *Inorg. Chim. Acta* **2007**, *360*, 1154.

[19] Geometry optimization and single-point DFT calculations have been carried out at the B3LYP/3-21G* level of theory in the gas phase as well as including the solvent (acetonitrile) by using the Tomasi's polarized continuum model (PCM) as implemented in Gaussian 03.

[20] M. J. Frisch, G. W. Trucks, H. B. Schlegel, G. E. Scuseria, M. A. Robb, J. R. Cheeseman, J. A. Montgomery Jr., T Vreven, K. N. Kudin, J. C. Burant, J. M. Millam, S. S. Iyengar, J. Tomasi, V. Barone, B. Mennucci, M. Cossi, G. Scalmani, N. Rega, G. A. Petersson, H. Nakatsuji, M. Hada, M. Ehara, K. Toyota, R. Fukuda, J. Hasegawa, M. Ishida, T. Nakajima, Y. Honda, O. Kitao, H. Nakai, M. Klene, X. Li, J. E. Knox, H. P. Hratchian, J. Cross, V. Bakken, C. Adamo, J. Jaramillo, R. Gomperts, R. E. Stratmann, O. Yazyev, A. J. Austin, R. Cammi, C. Pomelli, J. W. Ochterski, P. Y. Ayala, K. Morokuma, G. A. Voth, P. Salvador, J. J. Dannenberg, V. G. Zakrzewski, S. Dapprich, A. D. Daniels, M. C. Strain, O. Farkas, D. K. Malick, A. D. Rabuck, K. Raghavachari, J. B. Foresman, J. V. Ortiz, Q. Cui, A. G. Baboul, S. Clifford, J. Cioslowski, B. B. Stefanov, G. Liu, A. Liashenko, P. Piskorz, I. Komaromi, R. L. Martin, D. J. Fox, T. Keith, M. A. Al-Laham, C. Y. Peng, A. Nanayakkara, M. Challacombe, P. M. W. Gill, B. Johnson, W. Chen, M. W. Wong, C. Gonzalez, J. A. Pople, *Gaussian 03*, revision C.02, Gaussian, Inc., Wallingford CT, **2004**.

[21] a) R. O. Steen, L. J. Nurkkala, S. J. Angus-Dunne, C. X. Schmitt, E. C. Constable, M. J. Riley, P. V. Bernhardt, S. J. Dunne, *Eur. J. Inorg. Chem.* **2008**, 1784–1794; see also: b) J. L. Fillaut, J. Perruchon, P. Blanchard, J. Roncali, S. Golhen, M. Allain, A. Migalsaka-Zalas, I. V. Kityk, B. Sahraoui, *Organometallics* **2005**, *24*, 687–695.

[22] B. P. Sullivan, J. M. Calvert, T. J. Meyer, *Inorg. Chem.* **1980**, *19*, 1404–1407.

[23] W. Wilker, D. Leibfritz, R. Kesserbaum, W. Beimel, *Magn. Reson. Chem.* **1993**, *31*, 287.

[24] R. E. Hurd, *J. Magn. Reson.* **1990**, *87*, 422.

[25] a) *Antigona* is a program developed by Dr. Loïc Mottier, University of Bologna, Bologna, Italy, **1999**; b) B. Spieser in *Electroanalytical Chemistry. A Series of Advances*, vol. 19 (Eds: A. J. Bard, I. Rubistein), Marcel Dekker, Inc., New York, **1996**, p. 1.

[26] D. F. Eaton, *Pure Appl. Chem.* **1988**, *60*, 1107.

[27] G. M. Sheldrick, *SADABS*, Program for Empirical Absorption Correction, University of Göttingen, Germany, **1996**.

[28] G. M. Sheldrick, *SHELX97-Program for the Refinement of Crystal Structures*, University of Göttingen, Germany, **1997**.

[29] H. D. Flack, *Acta Crystallogr., Sect. A* **1983**, *39*, 876.

Received: April 13, 2010
Published Online: August 17, 2010

 © 2010 Wiley-VCH Verlag GmbH & Co. KGaA, Weinheim